UNIVERSITI PUTRA MALAYSIA

EFFECT OF COPPER OXIDE TO THE STRUCTURAL AND ELASTIC PROPERTIES OF ALUMINA MAGNESIUM LITHIUM SULPHOPHOSPHATE GLASS SYSTEM (Al2O3-MgO-Li2SO4-P2O5)

NUR HIDAYAH BINTI ZAIFUL AFENDY

EFFECT OF COPPER OXIDE TO THE STRUCTURAL AND ELASTIC PROPERTIES OF ALUMINA MAGNESIUM LITHIUM SULPHOPHOSPHATE GLASS SYSTEM (Al_2O_3-MgO-Li_2SO_4-P_2O_5)

By

NUR HIDAYAH BINTI ZAIFUL AFENDY

196711

Thesis Submitted to the Department of Physics, Universiti Putra Malaysia, in partial Fulfilment of the Requirement for the Degree of Bachelor of Science with Honours in Material Science

February 2022

DEDICATION

To my beloved parents Zaiful Afendy bin Omar and Rohana Binti Taib
For their love and support and always believing in me.

To my siblings and family
Where my life begins and loves never ends

To all my very wonderful friends
For brings sunshine, joy and always together in the spirit

To all my lecturers
For hard-working and helping me at a lot throughout this journey

Thank you all

ABSTRACT

EFFECT OF COPPER OXIDE TO THE STRUCTURAL AND ELASTIC PROPERTIES OF ALUMINA MAGNESIUM LITHIUM SULPHOPHOSPHATE GLASS SYSTEM

By

NUR HIDAYAH BINTI ZAIFUL AFENDY (196711)

February 2022

Supervisor: Dr. Mohd Hafiz Mohd Zaid

Department: Department of Physics

The production of copper alumina magnesium lithium sulphophosphate glasses at different compositions added according to the empirical formula $x(CuO)$-$5(Al_2O_3)$-$15(MgO)$-$20(Li_2SO_4)$-60-$x(P_2O_5)$ with x= 0, 0.2, 0.4, 0.6, 0.8 and 1.0 mol % was prepared by using the melt-quenching technique and investigated by X-ray diffraction (XRD), ultrasonic velocities, density, molar volume and the properties of the structural and elastic model. The experimental elastic moduli that used to investigate the elastic properties of glass was including longitudinal modulus, Young's modulus, bulk modulus, microhardness and Poisson's ratio. In this study, the Makishima and Mackenzie model was also discussed and explained more to investigate the theoretical elastic moduli of the glasses. XRD confirmed an amorphous CuO-Al_2O_3-MgO-Li_2SO_4-P_2O_5 glass structure, a broad halo peak at angle ≈ 20 ° - 28 ° and continuous sharp peak absent observed in glass system. The experimental results show that the

density of the glass sample increase from 2.500 to 2.522 g cm^{-3} and molar volume of the glass sample was decrease from 47.320 to 46.700 cm^3/mol. In addition, the result shown in experimental elastic moduli measurements, the values for the longitudinal (L) increase from 5011 to 5458 cm^{-1}, shear (G) increased from 3356 to 3664 cm^{-1}**,** bulk (K) increased from 25.18 to 29.93 GPa, Young's modulus (E) increased from 61.58 to 73.77 GPa, Poisson's ratio decreased 0.092 to 0.088 and microhardness increased from 7.669 to 9.312 GPa. As for Makishima-Mackenzie theory, the longitudinal modulus increased from 9.657 to 9.750 GPa, shear modulus increased from 6.673 to 6.741 GPa, bulk modulus increased from 7.600 to 7.623 GPa, Young's modulus increased from 4.831 to 4.854 GPa and lastly microhardness increased from 2.084 to 4.110 GPa and Poisson's ratio decreased from 0.086 to 0.061. The results of XRD, ultrasonic velocities and elastic moduli evidenced the formation of CuO-Al_2O_3-MgO-Li_2SO_4-P_2O_5 glass system and potentially used in the fields of sealing and laser glasses also in biomedical glasses.

ABSTRAK

KESAN KUPRUM OKSIDA TERHADAP SIFAT STRUKTUR DAN ELASTIK DARIPADA SISTEM KACA ALUMINA MAGNESIUM LITIUM SULFOFOSFAT

Oleh

NUR HIDAYAH BINTI ZAIFUL AFENDY
(196711)

Februari 2022

Penyelia: Dr. Mohd Hafiz Mohd Zaid

Jabatan: Jabatan Fizik

Penghasilan gelas alumina kuprum magnesium litium sulfofosfat pada komposisi berbeza ditambah mengikut formula empirik $x(CuO)$-$5(Al_2O_3)$-$15(MgO)$-$20(Li_2SO_4)$-60-$x(P_2O_5)$ dengan x= 0, 0.2, 0.4, 0.6, 0.8 dan 1.0 mol % telah disediakan dengan menggunakan teknik peleburan lebur dan disiasat oleh pembelauan sinar-X (XRD), halaju ultrasonik, ketumpatan, isipadu molar dan sifat-sifat model struktur dan elastik. Modul elastik eksperimen yang digunakan untuk menyiasat sifat elastik kaca adalah termasuk modulus membujur, modulus ricih, modulus Young's, modulus pukal, kekerasan mikro dan nisbah Poisson's. Dalam kajian ini, model Makishima dan Mackenzie turut dibincangkan dan diterangkan dengan lebih lanjut untuk menyiasat moduli elastic teori sampel kaca. XRD mengesahkan struktur kaca CuO-Al_2O_3-MgO-Li_2SO_4-P_2O_5 amorf, puncak halo luas pada sudut ≈ 20 ° - 28 ° dan puncak tajam berterusan tidak diperhatikan dalam sistem kaca. Keputusan eksperimen menunjukkan bahawa ketumpatan sampel kaca meningkat daripada 2.500 kepada 2.522 g cm-3 dan

isipadu molar sampel kaca berkurangan daripada 47.320 kepada 46.700 cm3/mol. Di samping itu, keputusan yang ditunjukkan dalam pengukuran moduli elastik eksperimen, nilai untuk peningkatan membujur (L) daripada 5011 kepada 5458 cm-1, modulus ricih (G) meningkat daripada 3356 kepada 3664 cm-1, modulus pukal (K) meningkat daripada 25.18 kepada 29.93 GPa, modulus Young's (E) meningkat daripada 61.58 kepada 73.77 GPa, nisbah Poisson menurun 0.092 kepada 0.088 dan kekerasan mikro meningkat daripada 7.669 kepada 9.312 GPa. Bagi teori Makishima-Mackenzie pula, modulus membujur meningkat daripada 9.657 kepada 9.750 GPa, modulus ricih meningkat daripada 6.673 kepada 6.741 GPa, modulus pukal meningkat daripada 7.600 kepada 7.623 GPa, modulus Young meningkat daripada 4.831 kepada 4.854GPa manakala nilai kekerasan meningkat dari 2.084 kepada 4.110 GPa dan nisbah Poisson menurun daripada 0.086 kepada 0.061. Keputusan XRD, kelajuan ultrasonik dan moduli elastik membuktikan pembentukan sistem kaca CuO-Al_2O_3-MgO-Li_2SO_4-P_2O_5 dan berpotensi digunakan dalam bidang meterai dan gelas laser juga dalam gelas bioperubatan.

ACKNOWLEDGEMENTS

In the name of Allah S.W.T, the Most Gracious and Most Merciful. First and foremost, I am very grateful to Him for the blessing to be able to complete my thesis work successfully.

First and foremost, I would like to express my deepest gratitude to my supervisor, Dr. Mohd Hafiz Mohd Zaid, for his patience, guidance and valuable advice regarding my project throughout my research. It was a tremendous privilege and honor to work and study under his supervision since it assisted in the success of my research.

Apart from that, my sincere appreciation to my senior, Nuraidayani Effendy for her encouragement, guidance, patience and emotional support throughout this research. She never hesitated to help and share her knowledge and experiences about the experimental and thesis work.

I also want to thank to all my fellow friends especially to Chen Zhe Ying and Izyan Fatihah binti Abdul Fatah for their invaluable discussion throughout the research work. Not to forget, Muhammad Amir Safwan bin Zamani Ahmad, Nur Syahmina binti Zulkifli and Nur Shafiqah Ridhani binti Mohd Sazeli for their endless support including emotional and physical support. Their prayer for me was what sustained me this far.

Lastly, I am extremely grateful to my family, Zaiful Afendy bin Omar, Rohana binti Taib and Muhammad Eiman bin Zaiful Afendy for their endless love, prayers and sacrifices for my future. My special thanks goes to them for their unconditional understanding and for sharing wisdom that inspires me to push beyond my limits and as well as giving their best for me.

APPROVAL

This thesis entitled "Effect Of Copper Oxide To The Structural And Elastic Properties Of Alumina Magnesium Lithium Sulphophosphate Glass System" by Nur Hidayah binti Zaiful Afendy (Matric No.: 196711), was submitted to the Department of Physics, Faculty of Science, Universiti Putra Malaysia and has been accepted as partial fulfillment of the requirement for the degree of Bachelor of Science with Honours in Material Science.

Approved by,

DR. MOHD HAFIZ BIN MOHD ZAID
Pensyarah Kanan
Jabatan Fizik
Fakulti Sains
Universiti Putra Malaysia
43400 UPM Serdang

Date: 7 August 2022 ……

Dr. Mohd Hafiz Mohd Zaid
Project Supervisor
Department of Physics
Faculty of Science
Universiti Putra Malaysia

Date: ……

Dr. Md Shuhazlly Mamat @
Mat Nazir
Course Coordinator
Department of Physics
Faculty of Science
Universiti Putra Malaysia

Date: ……

Assoc. Prof. Dr. Suriati Paiman
Head of Department
Department of Physics
Faculty of Science
Universiti Putra Malaysia

DECLARATION

I hereby confirm that:

- this thesis is my original work;
- quotations, illustrations and citations have been duly referenced;
- this thesis has not been submitted previously or concurrently for any other degree at any other institutions;
- intellectual property from the thesis and copyright of thesis are fully-owned by Universiti Putra Malaysia, as according to the Universiti Putra Malaysia (Research) Rules 2012;
- written permission must be obtained from supervisor and the office of Deputy Vice-Chancellor (Research and Innovation) before thesis is published (in the form of written, printed or in electronic form) including books, journals, modules, proceedings, popular writings, seminar papers, manuscripts, posters, reports, lecture notes, learning modules or any other materials as stated in the Universiti Putra Malaysia (Research) Rules 2012;
- there is no plagiarism or data falsification/fabrication in the thesis, and scholarly integrity is upheld as according to the Universiti Putra Malaysia (Graduate Studies) Rules 2003 (Revision 2012-2013) and the Universiti Putra Malaysia (Research) Rules 2012. The thesis has undergone plagiarism detection software.

Signature: …… Date: 7th August 2022

Name and Matric No.: Nur Hidayah Binti Zaiful Afendy (196711)

TABLE OF CONTENT

LIST OF TABLES

LIST OF FIGURES

LIST OF ABBREVIATIONS AND SYMBOLS

Cu	Copper
Mg	Magnesium
Ca	Calcium
Ba	Barium
UV	Ultraviolet
MgO	Magnesium oxide
CuO	Copper oxide
CaO	Calcium oxide
SiO_2	Silicon oxide
P_2O_5	Phosphorus pentoxide
Al_2O_3	Aluminium oxide
Li_2SO_4	Lithium sulphate
B_2O_3	Boron trioxide
XRD	X-Ray diffraction
OPD	Oxygen packing density
BO	Bridging oxygen
NBO	Non-bridging oxygen
DSC	Differential scanning calorimetry
DTA	Differential thermal analysis
ρ	Density
V_m	Molar volume
V_t	Packing density
Vo	Oxygen molar volume
V_L	Longitudinal ultrasonic velocity
V_S	Shear ultrasonic velocity
L	Longitudinal modulus
G	Shear modulus
K	Bulk modulus
E	Young's modulus

H	Microhardness
σ	Poisson's ratio
V_i	Packing density parameter
G_i	Dissociation energy
M_i	Molecular weight
G_t	Dissociation energy per unit volume

CHAPTER 1

INTRODUCTION

1.1 Research Background

Glass is a non-crystalline solid material and it is typically brittle. It is often optically transparent. Glass is an amorphous solid without a long range order (J.E.Shelby, 2005). Glass shows a glass transition as it has a condition where the solid amorphous phase shows a sudden change in terms of thermodynamics properties with a change in temperature. Glass is also an amorphous material that can be produced from melt quenching techniques (Celikbilek *et al*., 2013). Glass is a super cold liquid, which means it is stiff and static but does not shift molecularly between melting and solidifying into a particular shape. It is one of the most versatile materials on the planet, with a vast range of applications and shapes ranging from simple clear glass to tempered and coloured types and so on (Dtu & Io, 2011).

Phosphate glasses are important materials in both science and technology as they have unique physical properties that are superior to those of other glasses such as high thermal expansion coefficients, low melting and softening temperatures, high electrical conductivity and also have good ultraviolet (UV) transmission and optical properties (MINAMF & MACKENZIE, 1977). The chemical durability of phosphate glasses can be increased by adding different oxides, according to several research. Adding different metal oxides with high valence cations to alkali phosphate glasses

improves their physical qualities and chemical durability (Nie *et al.,* 2015). Displays, sensors, lasers, and amplifiers have all used phosphate glasses (Amarnath Reddy *et al.,* 2012).

Alkali sulphophosphate glasses, such as Li_2SO_4–P_2O_5, are recognized globally as sources for radioactive waste immobilisation (Sekhar *et al.,* 2020). Li_2SO_4 – P_2O_5 glasses are well known due to its extensive usage in ionic batteries as electrolytes. This is because of their large ionic current component contribution due to the diffusion of Li^+ ions (Scholz, 2011). MgO and other alkaline oxides are well-known modifiers in glass matrices, particularly in the phosphate glass network. These oxides are commonly used to improve the water durability of P_2O_5 glass systems (Prasad *et al.,* 2007).

Lithium sulphophosphate glasses was carried out using the melt quenching technique. XRD measurement was observed to investigate the structure of the materials which is amorphous based on diffraction pattern. The glass density, which is a capable attribute, was investigated in order to determine the compactness of the glass structure. The density value may be influenced by the structure's compactness, the space's interstitial dimension, and the number of glass coordination (Sidek *et al.,* 2013). Furthermore, ultrasonic velocities provide structural behavior knowledge inside the glass system, which is an important criteria for investigating elastic properties.

The longitudinal, shear, Young's, and bulk modulus, which are determined by Poisson's ratio were used to determine the characteristics of structural and elastic models. The elastic moduli, according to the Makishima and Mackenzie model take into consideration the energy dissociation per unit volume (G_t) and packing density (V_t) with chemical compositions of oxide glasses. Lastly, the objective of this study is to study the effect of copper oxide to the structural and elastic properties of alumina magnesium lithium sulphophosphate glass system.

1.2 Problem Statement

Phosphate glass, P_2O_5 is a glass former because it can form single component of glass by itself (Dtu & Io, 2011). It also helps to improve the properties of the glass by adding a glass modifier or an intermediate glass into the glass system. Glass modifiers change the coefficient of thermal expansion, chemical durability, and refractive index of the material, making it simpler to work with at lower temperatures while maintaining transparency (Mo-Sci Corp., 2020). The intermediate glass will improve the glass system by increase the thermal expansion coefficients of the glass system (Saddeek *et al*., 2016). Copper oxide, CuO has been chosen by several studies to be used as a glass modifier as it is good in semiconductor properties. In addition, aluminium oxide, Al_2O_3 as a glass intermediate because it has a good shielding properties(Kaur *et al*., 2019).

The latest research was to investigate the effect of copper ions on the dielectric properties and ac conductivity of lithium sulpho magnesium phosphate glasses. Technique use to analyse the structural properties of the glass also different as they

use XPS, optical absorption (OA) and IR spectra (Sekhar *et al.*, 2020). There are limitations of study on effect of the copper oxide to the structural and elastic properties of alumina magnesium lithium sulphophosphate glass system. Therefore, this study will go further on the preparation and characterization of the copper oxide and how this material will affect the structural and elastic properties of alumina magnesium lithum sulphophosphate glass system.

1.3 Objectives

The purpose of this project is to study the impact of copper oxide on the structural and elastic properties of Al_2O_3-MgO-Li_2SO_4-P_2O_5 glass. The most important technique in the fabrication of this glass were melt quenching method, CuO as an addition and the studies from XRD, density, molar volume, ultrasonic velocities and the properties of structural and elastic model.

The objectives of this analysis are mentioned below:

1. To synthesize CuO-Al_2O_3-MgO-Li_2SO_4-P_2O_5 glass using conventional melt-quenching method.
2. To determine the effect of CuO to the structural and elastic properties of Al_2O_3-MgO-Li_2SO_4-P_2O_5 glass system.
3. To investigate the correlation between Makishima and Mackenzie model to the elastic properties of alumina magnesium lithium sulphophosphate glass system.

1.4 Scope of study

There are some scope of study as follows:-

1) Glass preparation using some raw material such as CuO, Al_2O_3, MgO, Li_2SO_4 and P_2O_5 powder based using empirical formula x(CuO)-5(Al_2O_3)-15(MgO)-20(Li_2SO_4)- 60-x(P_2O_5)
   (x= 0, 0.2, 0.4, 0.6, 0.8 and 1.0 mol %) by melt-quenching technique.

2) Analyze structural and elastic properties of CuO-Al_2O_3-MgO-Li_2SO_4-P_2O_5 glass samples using XRD, ultrasonic velocities and Makishima and Mackenzie model.

1.5 Outline of the thesis

For this thesis, there are five chapters included followed by the well organized sequence. In chapter 1, there are 4 sections included which are research background, discuss the problem statements, the main purpose of the study and the significance of this study that explain why this research was needed also provided. In chapter 2, literature review, it gave a broad overview of structural and elastic investigations. It also described the structure and the behavior of copper oxide to the Al_2O_3-MgO-Li_2SO_4-P_2O_5 glass system.

In chapter 3, this chapter explains the details of the method and procedures used to prepare the glass also the technique used in this research has been discussed. Last but not least, the experimental result that has been analyzed were discussed in chapter 4

concerning the effect of CuO that were added in Al_2O_3-MgO-Li_2SO_4-P_2O_5 glass, the progress of melt-quenching method and different mol percentage (%) of CuO added to the structural and elastic properties of CuO-Al_2O_3-MgO-Li_2SO_4-P_2O_5 glass system. Lastly for chapter 5, the conclusion and some suggestion for upcoming study were presented

CHAPTER 2

LITERATURE REVIEW

2.1 Introduction

The second chapter of this thesis contained a detailed analysis of glass. Firstly, research began with broad review of glass before proceed to the oxide glass. The discussion is then broadened to include information on phosphate glass, lithium sulphophosphate glass and copper oxide in magnesium lithium sulphophosphate glass.

2.1.1 Glass

Glass is known as a non-crystalline solid material. It is brittle and usually hard amorphous solids (Mahan *et al*., 2019). Glass also have a high tensile strength and also can be pour, form, mold and extrude (Saloumi *et al.,* 2019).he It is a mechanically strong as when it subjected to significant temperature change, and has a hard surface that resists abrasion and corrosion in its ideal form. Glass is also act as elastomer as it can yield under stress up to its breaking point and then will bounce back to its original shape (Ahmad *et al.,* 2020). Glass is divided into three categories of components which are glass former, glass modifier and lastly, glass intermediate. Their characteristics of glass will change when different glass components are used.

2.1.2 Glass Former

Majority glass is made up of network formers which create a strongly cross-linked network of chemical bond (Calahoo & Wondraczek., 2020). Glass former may be considered as the glass backbone and modifying this element or compound will have a significant impact of the final product (Ahmad *et al.,* 2020). The glass former is always the most crucial component of every glass batch. The most frequent network-forming component of glass is silicon oxide (SiO_2), other oxides as example germanium and boron are also often used in the industry based on their oxides (Ahmad *et al.,* 2020). Silica glass is used in applications that require a high service temperature, extremely high thermal shock resistance, great chemical durability, extremely low electrical conductivity and also good UV transparency (Varshneya., 2016). There are more other conventional glass formers such as P_2O_5 and B_2O_3 (Banerjee., 2011).

2.1.3 Glass Modifier

Modifier are additives that can be used to change the properties of glass in a small amount which known as property modifier. For example, alkaline earth such as Magnesium (Mg), calcium (Ca), barium (Ba) and many more transition metal oxide such as copper (Cu) and alkali oxides are also example for glass modifier. Cavities in the glass network are filled by alkaline earth elements, which are found in abundance. Bonds between alkaline earth ions and oxygen are strong compared to alkali metals.

This will affect their properties such as lowering the melting temperature and viscosity by reducing the relative number of strong connections in the glass.

2.1.4 Glass Intermediate

Intermediates, such as titanium, aluminium, and zirconium oxides, are compounds that depending on the glass composition, can act as network-formers or modifiers (Granados *et al.*, 2021). It cannot form glass network by themselves but can join into existing network Glasses are naturally very disordered, and preventing the creation of ordered crystallites within the material necessitates a finely adjusted mix of network formers, intermediates, and modifiers. With temperature and/or pressure, intermediate glasses have virtually constant elastic moduli. These glasses might be used to create a-thermal optical fibers for improved communications, fiber sensing applications, and glass goods for applications that need a wide range of heat and mechanical stimulation (Jaccani *et al*., 2018).

2.2 Phosphate Glass, P_2O_5

Phosphate glass has been studied for nearly a century and a half. Despite the fact that P_2O_5 is one of the four classic Zachariasen glass forming oxides (together with SiO_2, B_2O_3, phosphate glass application has been limit due to its hygroscopic nature. Phosphate glass are made up of P_2O_5 with the addition of CaO and Na_2O as a modifier (Brow., 2000).

Phosphate glass is a glass former because technologically, it is a crucial material because of their relatively high thermal expansion coefficient, low optical dispersion and low glass transition temperature (T_g). However, it is also relatively have a poor chemical durability which will limit their applications. By adding various oxides to phosphate glasses such as ZnO, CuO, Al_2O_3 and many more will help to increase their chemical durability (Ahmina *et al.,* 2016).

Phosphate glass application have been limit due to its hygroscopic nature. This glass have a huge transmission in the ultraviolet region, low thermo-optical coefficient and large emission compared to the silicate glasses so it is the right material for high power laser. Due to their low melting temperature, low viscosity and high thermal expansion coefficients, phosphate glasses are suitable as glass-metal seals.

2.3 Lithiumsulpho- Phosphate Glass, Li_2SO_4-P_2O_5

Various authors have conducted several investigations on various glassware and glass-ceramic systems along similar lines in the recent past, many of which have given significant information (Zhang *et al.,* 2020). Furthermore, studies on the electrical properties of amorphous electrolytic materials with a low concentration of transition metal ions, such as lithiumsulpho-phosphate glasses, are extremely useful in determining their suitability as a cathode in electrochemical cells (Lim *et al.,* 2018).

Despite the fact that the S–O bond length in sulphate units and the P–O bond length in phosphate units are approximately the same, recent quantitative investigations have suggested that the potential of links between phosphate and sulphate units (P–O–S) forming in the glass network is very low. As a result, the structural disorder in the sulphophosphate glass around SO_4^{2-} ions is extremely high. Sulphate ions (SO_4^{2-}) have a high miscibility in phosphate glasses, according to reports. Nonetheless, dissolution of these ions in metaphosphate glasses was shown to be very weak, and new structural units known as dithiophosphate are projected to form in such glasses (Da *et al.*, 2011).

2.4 Alumina in Phosphate Glass

According to Filho *et al.,* (2020) it has long been known that adding Al_2O_3 to phosphate glass changes the glass characteristics in ways that indicate more structural polymerization. By adding Al_2O_3, for example, the expansion coefficient is reduced, T_g is increased, and chemical durability is improved. Aluminium oxide, Al_2O_3 is commonly used as an intermediate glass so it can either act as a glass former or a glass modifier. It depends on the concentration of the glass composition. When Al_2O_3 was added into the glass network , the properties of glass network and also its energy gap may be change (Saddeek *et al.*, 2016).

2.5 Elastic Moduli Model

The Makishima-Mackenzie (MM) model, which was developed theoretically, explains the Young modulus of glass in terms of interatomic bonding strength (dissociation energy) and the behavior in which atoms are packed (atomic packing fraction) (Shi *et al.,* 2020). This model provides a clear physical image of the compositional dependence of glass stiffness, but it significantly underestimates the true Young's modulus for many glasses, particularly in the high value range. Based in the chemical composition of the glass and the atom packing density (V_t), bond energy per unit volume or dissociation energy (G), they derived applicable semi-empirical method for calculating Young's modulus and Poisson's ratio (Saddeek *et al.,* 2016).

CHAPTER 3

METHODOLOGY

3.1 Introduction

This section in this thesis explained in details the procedure to prepare and characterize the copper oxide in alumina magnesium lithium sulphophosphate glass system and it has been prepared by using conventional melt-quenching method. Besides, mixing the raw ingredients and quenching the melt glass process were needed to produce glass. The next part is characterization, it explains the techniques used to determine the properties of the glass itself. In addition, their physical, structural and elastic properties will be analyzed in this part. Many techniques that has been used in this part such as XRD, density, molar volume, ultrasonic velocities, elastic modulus and Makishima-Machenzie model.

3.1.1 Sample preparation

The glass sample has been prepared by using conventional melt-quenching technique. The experiment was begin with weight and mix the pure chemicals and end with polish and grinding before determine its properties. During quenching process, the cooling process need to be carried out immediately to maintain their properties.

In this study, CuO, Al_2O_3, MgO, Li_2SO_4 and P_2O_5 were used as raw materials to prepare the glass. All the raw materials stated were weighting using a digital analytical balance based on an empirical formula x(CuO)-5(Al_2O_3)-15(MgO)-20(Li_2SO_4)- 60-x(P_2O_5) (x= 0, 0.2, 0.4, 0.6, 0.8 and 1.0 mol %) by melt-quenching technique with total weight of 30g for each glass. The digital analytical balance has an accuracy ± 0.1 mg. The values of chemical composition based on the empirical formula as shown in **Table 3.1.**

Table 3.1 Details composition of the CuO-Al_2O_3-MgO-Li_2SO_4-P_2O_5 glass samples (mol.%)

Glass samples	**CuO**	**Al_2O_3**	**MgO**	**Li_2SO_4**	**P_2O_5**
G1	0	5	15	20	60.0
G2	0.2	5	15	20	59.8
G3	0.4	5	15	20	59.6
G4	0.6	5	15	20	59.4
G5	0.8	5	15	20	59.2
G6	1.0	5	15	20	59.0

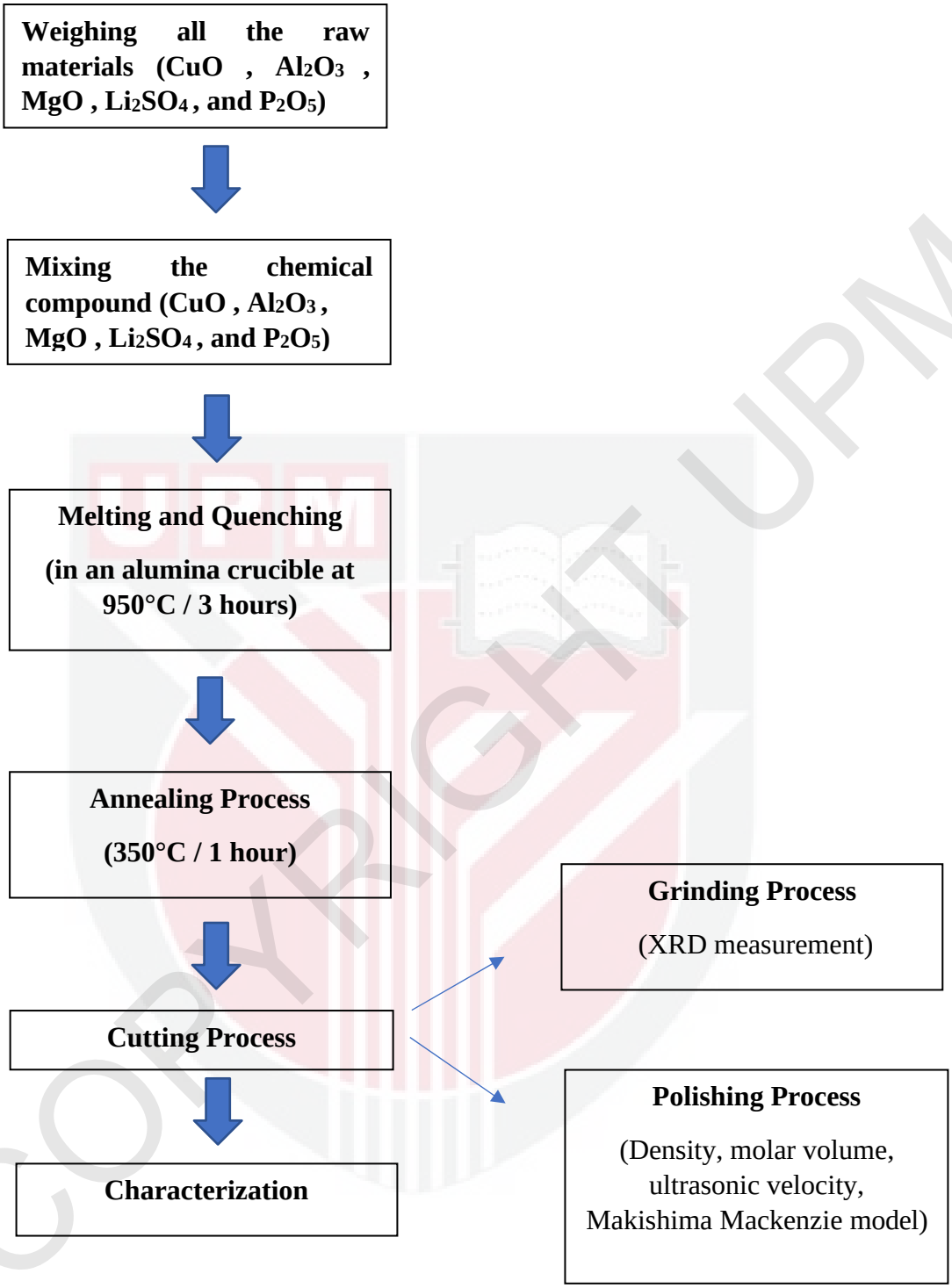

Figure 3.1 Schematic diagram for melt-quenching technique.

Firstly, the raw materials CuO, Al_2O_3, MgO, Li_2SO_4 and P_2O_5 were weighted by using a digital analytical balance that has an accuracy 0.001 g. All the raw materials were mixed together until it becomes homogeneous and being transferred into an alumina crucible and then placed in the electrical furnace to undergo melting process at 950 °C around about 3 hours to trapped any water vapor left (trapped) in the mixture have to be evaporated. Then, the melt poured onto stainless steel split mold by using long crucible tongs and cast it into a rectangular mold that had been preheat at 250°C around 1 hour. Next, the glass sample was transferred into an annealing furnace to proceed to an annealing process for about 1 hour at 350°C to prevent from thermal shock that can affect the sample to be crack and proceed to slowly cool it to room temperature. Lastly, analyzing the sample properties can be made after the sample undergo cutting, polishing and also grinding process.

3.2 X-Ray Diffraction (XRD) measurement

XRD is a flexible, non-destructive method for obtaining detailed qualitative and quantitative information regarding crystalline phases, chemical content, and crystallographic structure of natural and natural materials. XRD helps to identify the glass structure (in powder form) whether it is crystalline or in amorphous form. As for this study, the glass samples were measured in powder forms and XRD result appear in diffractogram form. Diffractogram form may reveal the glass structure, crystal orientation, crystal defects crystallinity and also its phases whether phase present and also phase concentration. The material is evaluated as a powder with grain in random orientations to ensure that the beam exposes all crystallographic directions. Using

Bragg's law, monochromatic X-rays are utilized to calculate the interplanar spacing of an unknown material. The Bragg's law can be expressed by:

$$n\lambda = 2d\sin\theta \tag{3.1}$$

Where n is an integer, λ is the wavelength of the X-rays, d is the interplanar spacing between the lattice plane of the crystal and θ is the diffraction angle between the incident ray and the scattering planes. The major objective of applying Bragg's rule is to determine the angle of constructive interference that is battered by X-rays that generate the diffraction peak by parallel planes of atoms. The d-spacing of a crystal is also employed for purposes of identification and categorization. Inter-planar spacing is the distance between the atoms' crystal lattice planes, which causes constructive interference (d-spacing).

3.3 Density

Density is a measurement used to calculate a body's or substance's mass from its volume. The density is measured in grammes per cubic centimeter (g/cm^3) and is derived using the formula mass per unit volume.

The fluid displacement method, which is based on the Archimedes principle, is commonly used to determine density. The buoyancy matches the weight of the displaced fluid, according to the Archimedes principle. The density of the glass samples was determined using the Archimedes Principle and xylene as the buoyant

medium. The density was calculated using the following formula (Chanshetti *et al.*, 2011):

$$\rho_g = \frac{w_a}{w_a - w_w} \times \rho_w \tag{3.2}$$

Where w_a and w_b are the sample of glass weight in air and water and $\rho_w = 1.00 g/cm^3$ is the density of water. The density, unlike the molar volume, rises as the CuO concentration increases. Cu and Na have different atomic weights, which explains this. When Al_2O_3 is added, the density decreases somewhat while the molar volume increases dramatically (Elbashar *et al.*, 2016).

3.4 Molar Volume

The volume of one mole of a material at a certain pressure and temperature is known as molar volume. The sign V_m is widely used to represent it. It is computed by multiplying the molar mass by the density, and it is measured in centimeter cubic per molar. The molar volume is directly proportional to the molar mass and inversely proportional to the density, according to the formula.

The molar volume (V_m) has been calculated using the following equation:

$$V_m = \Sigma \frac{x_i m}{\rho} \tag{3.3}$$

The oxygen molar volume (Vo) has been calculated using the following formula:

$$Vo = V_m \left(\frac{1}{\sum x_i n_i}\right) \tag{3.4}$$

The oxygen packing density (OPD) was calculated using the formula below:

$$OPD = 1000N \left(\frac{\rho}{M}\right) \tag{3.5}$$

Where x_i is molar fraction of oxides in the composition, m is molar mass of oxides and ρ is density of each oxide present in the glass composition, n_i is the amount of oxygen atoms for each of the constituent oxides, M is the molecular mass of the glass sample and N is the number of oxygen atoms in each composition (Zamyatin *et al.*, 2018).

3.5 Ultrasonic Velocity Measurement

At room temperature, ultrasonic velocity measurements were taken to investigate the microstructural changes in the glass network system. To put it another way, the ultrasonic measurements velocity is the speed of sound waves that pass between two parallel surfaces of glass samples. This pulse displays on the screen of a flaw detector employing the Ultrasonic Data Acquisition System (RITEC RAM-5000 S) generated by a typical electrical circuit. Using the Probe model as a NAP: The time pulse came out of a ceramic transducer on the OLYMPUS A109S-RB, which worked concurrently as a transmitter and receiver with resonance frequencies of 5 MHz. The SI unit for the ultrasonic velocity is meter per second (m/s). The following methods can be used to determine ultrasonic velocity reactions:

$$v = \frac{2d}{\Delta t} \tag{3.6}$$

Where d is the thickness of glass samples (in cm) and Δt is the time interval among the glass samples (s). For the velocity's measurement, estimation accuracy of shear velocity was ±0.011 ms^{-1} meanwhile longitudinal velocity was ±0.013 ms^{-1} (Effendy *et al.,* 2020).

3.6 Elastic Moduli Determination

Through the relationship between density and ultrasonic velocity measurement, the elastic modulus of longitudinal, shear, bulk, and Young's glass samples, as well as the Poisson's ratio, may be determined (Zaid *et al.*, 2021):

Longitudinal modulus, $L = \rho V_L^2$ (3.7)

Shear Modulus, $G = \rho V_S^2$ (3.8)

Bulk Modulus, $K = L - (\frac{4}{3})G$ (3.9)

Young's Modulus, $E = 2(1+\sigma)G$ (3.10)

Poisson's Ratio, $\sigma = \frac{L - 2G}{2(L - G)}$ (3.11)

Microhardness, $H = \frac{(1 - 2\sigma)E}{6(1 + \sigma)}$ (3.12)

Where ρ is refer to the glass samples density, V_L is the longitudinal ultrasonic velocity, V_S is refer to the shear ultrasonic velocity.

3.7 Makishima and Mackenzie Model

Makishima and Mackenzie developed a theoretical model that can be used to compute the elastic properties of inorganic oxide glasses based on their chemical compositions and density measurements. This model was also utilised to calculate stiffness and data correlation with the glass system's composition. In terms of dissociation energy per unit volume (G_t), and packing density (V_t), which represent the elastic moduli and Poisson's ratio of multi-component oxide glasses (Abd El-Moneim & Alfifi, 2018):

Young Modulus, $E_{MM} = 8.36\, V_t G_t$ (3.13)

Bulk Modulus, $K_{MM} = 10 V_t^2 G_t$ (3.14)

Shear Modulus, $G_{MM} = \frac{3K_M}{(10.2V_t - 1)}$ (3.15)

Longitudinal Modulus, $L_{MM} = K_{MM} + \frac{4}{3} G_{MM}$ (3.16)

Poisson's Ratio, $\sigma_{MM} = 0.5 - \frac{1}{7.2V_t}$ (3.17)

Microhardness, $H_{MM} = \frac{(1-2\sigma)E_{MM}}{6\,(1+\sigma_{MM})}$ (3.18)

Where G_t is the dissociation energy of oxide constituents per unit volume, x_i is the mol fraction of oxides component, and V_t the packing density of the glasses that obtained from the following equation for oxide (A_xO_y):

Packing density, $V_t = \sum_i \frac{V_i x_i}{V_m}$ (3.19)

Dissociation energy per unit volume, $G_t = \sum_i G_i x_i$ (3.20)

Packing factor, $V_i = \frac{4}{3} \pi N_A \left(X r_m^3 + Y r_o^3 \right)$ (3.21)

where r_m and r_0 both respectively is ionic radius of metal and oxygen based on the Pauling's ionic radii.

The Makishima–Mackenzie model uses two parameters to calculate Young's modulus which are bond strength and atomic packing. The model makes the reasonable assumption that bulk stiffness is proportional to bond strength and density, and attempts to represent this behavior by calculating bond strength from dissociation energy and bond density. The atomic packing fraction and the specific bond energy were combined to produce this result. Although the atomic packing fraction is the essential point at which glass structure enters the model, this description averages out aspects of intermediate range order (Plucinski & Zwanziger, 2015).

CHAPTER 4

RESULT AND DISCUSSION

4.1 Introduction

The structural and elastic properties of the glass samples were examined in this chapter. The series of glasses with empirical formula x(CuO)-5(Al_2O_3)-15(MgO)-20(Li_2SO_4)-60-x(P_2O_5) where x = 0, 0.2, 0.4, 0.6, 0.8 and 1.0 mol % were prepared using the melt quenching technique. Each glass sample was transparent, homogeneous and free of bubbles. The precursor glass series has been successfully prepared. XRD, ultrasonic velocities, density, molar volume and the properties of structural and elastic models were used to investigate the glass formation behavior and structural and elastic characteristics. The obtained results and glass's characterization are presented.

4.2 Structural Properties

4.2.1 X-ray Diffraction (XRD) Analysis

The X-ray diffraction patterns of the CuO-Al_2O_3-MgO-Li_2SO_4-P_2O_5 glasses is represented in **Figure 4.1** with different amount of CuO content. From **Figure 4.1**, There was a broad halo peak at a lower angle of 20°–28° and no continuous sharp peak, indicating that the most prominent feature is the amorphous structure (Abed *et al.*,

2021). It is clear from this that there is no long-range atomic order in the glass samples, but there is short-range atomic order present in the glass samples.

From **Figure 4.1** it can be seen as the CuO content increased, the broad peak shifted from a lower diffraction angle (20°) to a higher angle around (28°) and became less broadening. The rapid cooling method of the glasses from the melt is one of the reasons for missing crystallization and resulting in random amorphous distribution. The quenching method reduces both the nucleation and the growth of grain boundaries (Abed *et al.*, 2021).

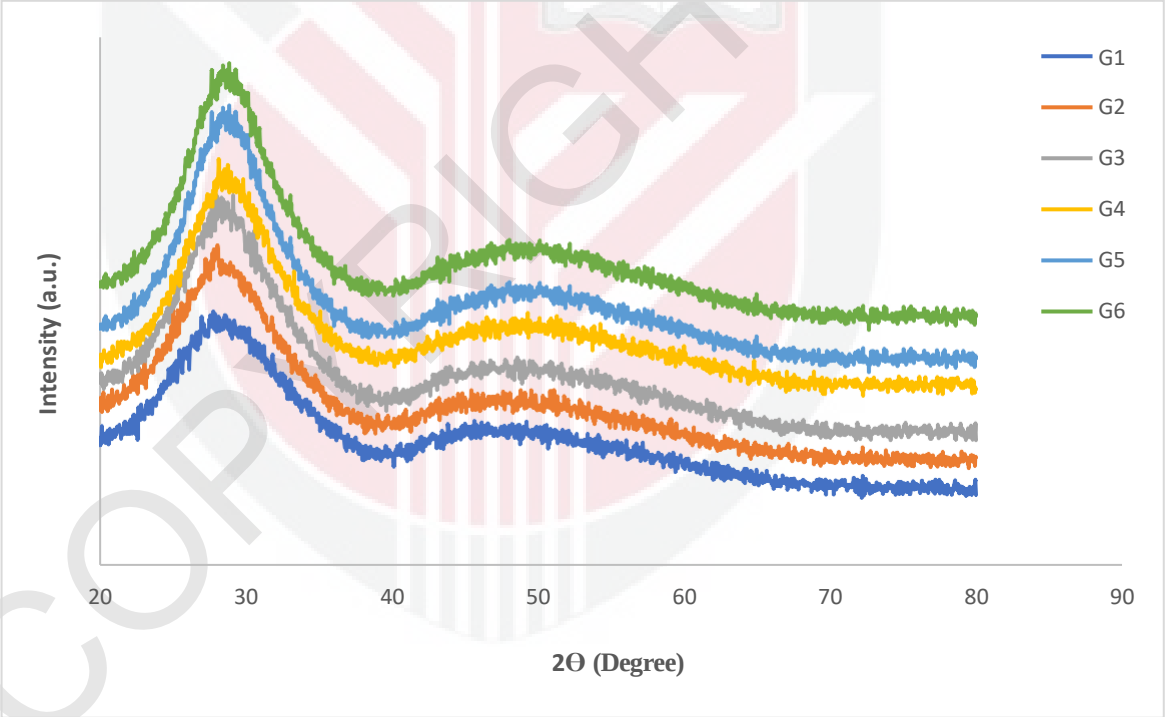

Figure 4.1 X-ray diffraction pattern of CuO-Al_2O_3-MgO-Li_2SO_4-P_2O_5 glass system

4.3 Physical Properties

4.3.1 Density, molar volume and oxygen packing density (OPD)

A series of CuO-Al_2O_3-MgO-Li_2SO_4-P_2O_5 pure powder were successfully melted and formed into a glass via conventional melt and quenching method. Glass density (ρ) is a way to measure how compact glass structures are. The density of a glass is an important property capable of evaluating the compactness and short-range structure of the glass. The increase in density is caused by a change in the glass structure caused by a decrease in interatomic spacing, which can be attributed to an increase in interatomic forces between the modifying cations and the glass forming anions inside the glassy network. As a result, the glass sample may become more compact and dense (Matori *et al.,* 2017).

The density (ρ), molar volume (V_m) and oxygen packing density (OPD) of glass samples are tabulated in in **Table 4.1**. The density of the copper alumina magnesium lithium sulphophosphate glasses increased from 2.500 to 2.522 g cm^{-3} as the concentration of CuO increased from 0.2 to 1.0 mol% as shown in **Figure 4.4**. The increasing of density is due to the replacement of P_2O_5 with copper oxide and its molecular weight of CuO (6.31 g/cm^3 and 79.54 g/mol). Density increase is also linked to the development of new connections caused by the addition of CuO, which results in volume shrinkage (Matori *et al.,* 2017). According to the literature, replacing CuO for P_2O_5 should result the decrease in density due to the lower molecular weight of CuO than P_2O_5 (M_{CuO} = 79.55gmol^{-1} ; $M_{P_2O_5}$ = 141.94 gmol^{-1}). The rise in density (as shown in **Figure 4.1**) implies that the copper ions are reticulating the network of glass molecules. This conclusion necessitates an examination of molar volume changes of

x (CuO)-5(Al_2O_3)-15(MgO)-20(Li_2SO_4)- 60- x (P_2O_5) glasses as a function of x (**Figure 4.1**).

The molar volume decreased from 47.32 to 46.66 cm^3 mol^{-1}. The densities and molecular weights of the glasses were used to calculate their molar volume. The decrease in molar volume as CuO content increases demonstrates that copper does reticulate the network. This effect is frequently observed when the concentration of a modifier oxide in metaphosphate glasses is increased. The density change of such systems is proportional to the density of the newly created structural units caused by the modifier oxide introduction (Elhaes *et al.*, 2014). Because CuO is a modifier glass, more non-bridging oxygens (NBOs) are formed in the glass network, and more Cu2+ ions occupy the spaces between atoms within the glass network. Additionally, some research has been investigated that a rise in the amount of non-bridging oxygen (NBO) is caused by the introduction of Cu cations into the network, which results in an open structure glass network (Morshidy *et al.*, 2020).

Table 4.1 Density (ρ), molar volume (V_m), packing density (V_t), oxygen molar volume (V_o) and oxygen packing density (OPD) of the CuO-Al_2O_3-MgO-Li_2SO_4-P_2O_5 glass system.

Glass Sample	Molar Percentage (mol.%)				
	Density, ρ (g/cm^3)	**Molar Volume, V_m (cm^3/mol)**	**Packing density, V_t**	**Oxygen molar volume, Vo (cm^3/mol)**	**OPD (mol/cm^3)**
G1	2.500	47.32	0.9326	15.643	86.65
G2	2.504	47.20	0.9291	16.011	86.57
G3	2.512	47.00	0.9248	16.121	85.90
G4	2.517	46.90	0.9206	16.323	83.65
G5	2.520	46.74	0.9173	17.931	83.20
G6	2.522	46.70	0.9146	17.366	81.03

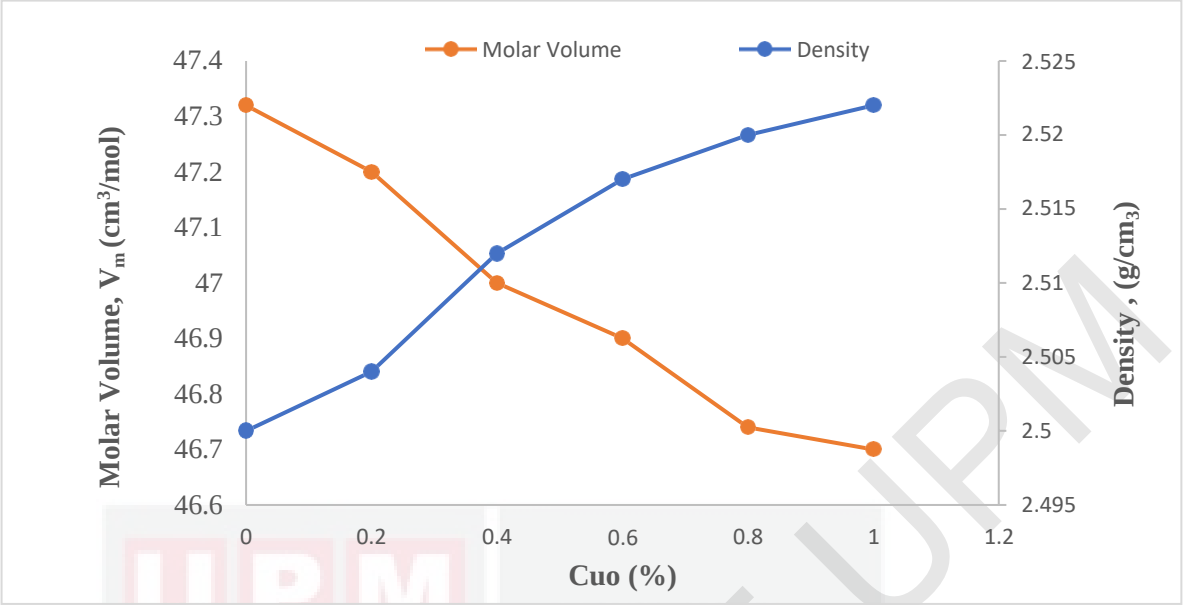

Figure 4.2 Density, (ρ) and molar volume, (V_m) of the CuO-Al_2O_3-MgO-Li_2SO_4-P_2O_5 glass system.

A plot of oxygen packing density (OPD) and oxygen molar volume (V_o) of CuO-Al_2O_3-MgO-Li_2SO_4-P_2O_5 glass sample is shown in **Figure 4.3**. It shows that the value of OPD is decreased from 86.65 to 81.03 mol cm^{-3} while for V_o the value is increased from 15.643 to 17.366 cm^3 mol^{-1} as the CuO content are increased from 0 to 1 mol% for this glass system. The OPD and V_o are in opposite trend to each other. This polar opposite trend in OPD and V_o may be due to the replacement of P_2O_5 with CuO as the network glass system becomes more compact and dense (Sayyed *et al.*, 2018). OPD decreases as CuO content is added to the structure. This variation indicated that the number of non-bridging oxygen (NBO's) increased as a result of the cleavage of P–O–P bridges during the progressive incorporation of CuO oxide (Oueslati-Omrani & Hamzaoui, 2020). It can be concluded from this that the glasses become increasingly tightly packed as the concentration of CuO increases (Elbashar *et al.*, 2016).

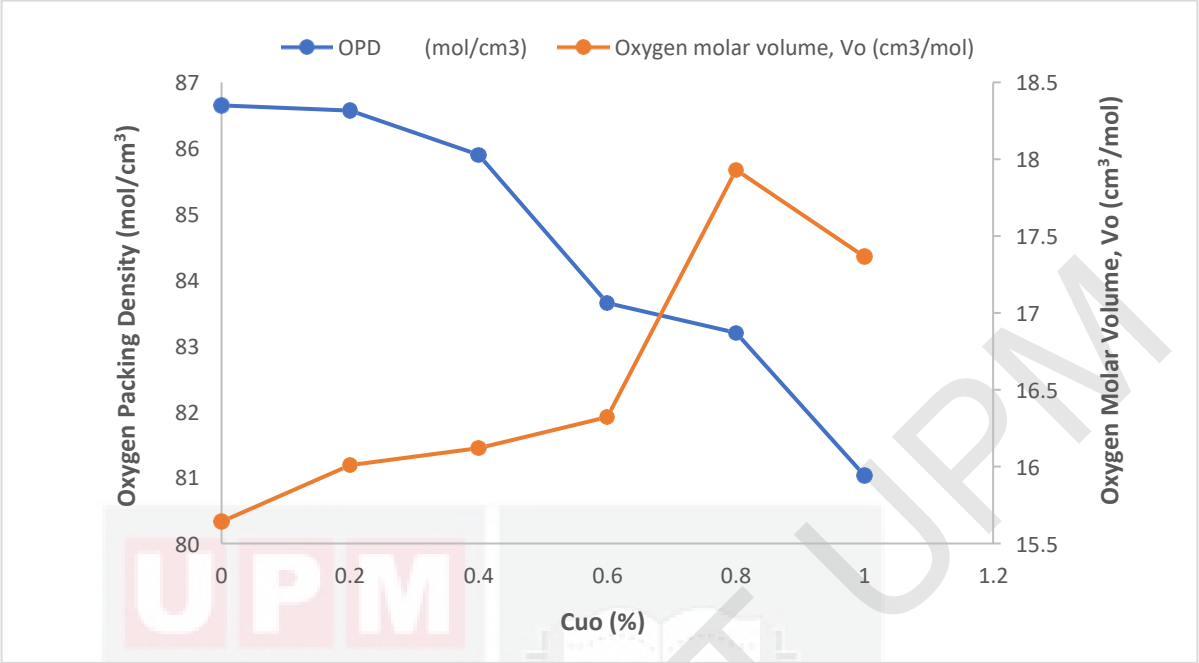

Figure 4.3 Oxygen packing density (OPD) and Oxygen molar volume (V_o) of the $CuO\text{-}Al_2O_3\text{-}MgO\text{-}Li_2SO_4\text{-}P_2O_5$ glass system

4.4 Elastic Properties

4.4.1 Elastic Properties of Copper Alumina Magnesium Lithium Sulphophosphate Glass

Ultrasonic velocities investigations are significant in explaining variations in the structural behavior of network glasses composition. The elastic modulus (L_{EXP}, G_{EXP}, K_{EXP} and E_{EXP}) was computed using the measured density and ultrasonic velocities. The longitudinal and shear ultrasonic velocities were determined experimentally using the pulse-echo method at room temperature and a resonating frequency of 5 MHz. Then, the microhardness (H_{EXP}) and Poisson's ratio (σ_{EXP}) were computed from the determined elastic modulus. The experimental elasticity modulus values and their respective theoretical values were computed to those calculated using the Makishima-Mackenzie model.

4.4.2 Elastic Modulus and Ultrasonic Velocities

Table 4.2 and **Figure 4.4** shows that the value of shear (V_S) and longitudinal (V_L) ultrasonic velocities both increased from 3356 ms^{-1} (0 mol%) to 3664 ms^{-1} (1 mol%) and from 5011 ms^{-1} (0 mol%) to 5458 ms^{-1} (1 mol%) when the glass network is added with the CuO content. The increase in ultrasonic velocity of the studied glass demonstrated that the addition of copper oxide results in a rapid movement of the ultrasonic wave within the glass structure's network. As the copper oxide content of the glasses increased, the ultrasonic velocity of the glasses increased as well. Copper oxide would form the glass structure, thereby increasing the hardness of the glass (Saddeek *et al.,* 2015). The values of the experimental results of longitudinal (L_{EXP}), shear (G_{EXP}), bulk (K_{EXP}), Young's (E_{EXP}) modulus, microhardness (H_{EXP}) and Poisson's ratio (σ_{EXP}) are listed in **Table 4.3** for CuO-Al_2O_3-MgO-Li_2SO_4-P_2O_5 glasses. The results show in **Figure 4.6** that the values L_{EXP}, G_{EXP}, K_{EXP}, E_{EXP} and H_{EXP} increase with increasing CuO content.

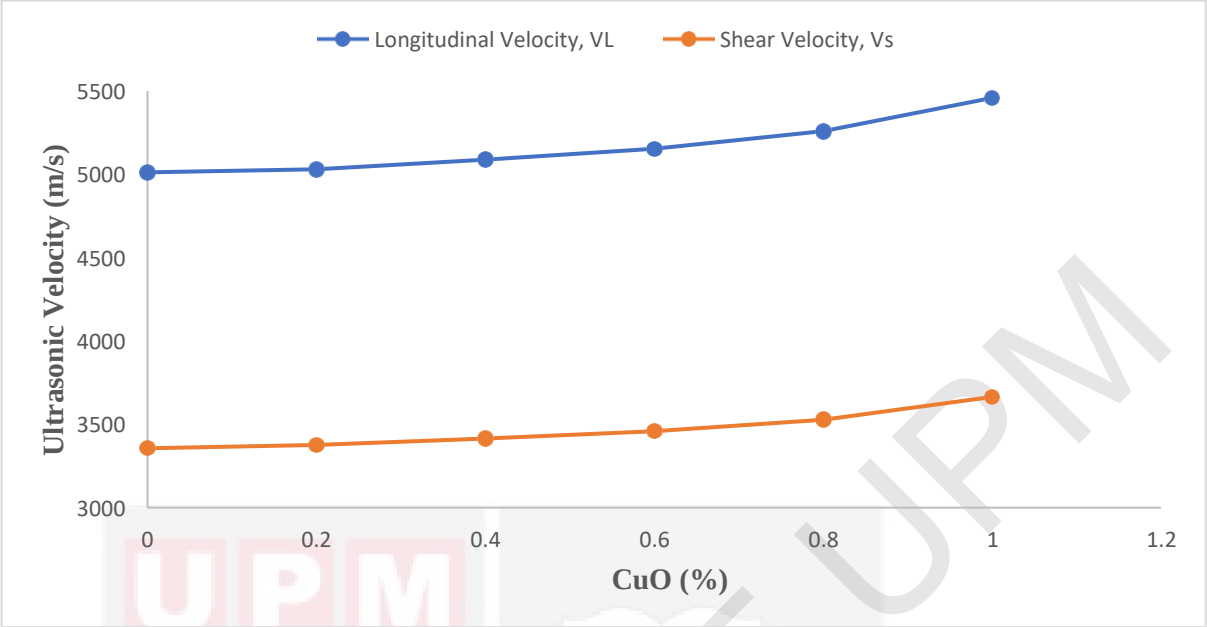

Figure 4.4 Ultrasonic velocities Longitudinal (V_L) and shear (V_S) of the CuO-Al_2O_3-MgO-Li_2SO_4-P_2O_5 glass system

Table 4.2 The longitudinal (V_L) and shear velocities (V_S) of the CuO-Al_2O_3-MgO-Li_2SO_4-P_2O_5 glass system

Glass Sample	CuO (mol%)	V_L (m/s)	V_S (m/s)
G1	0	5011	3356
G2	0.2	5030	3375
G3	0.4	5087	3414
G4	0.6	5153	3458
G5	0.8	5258	3528
G6	1.0	5458	3664

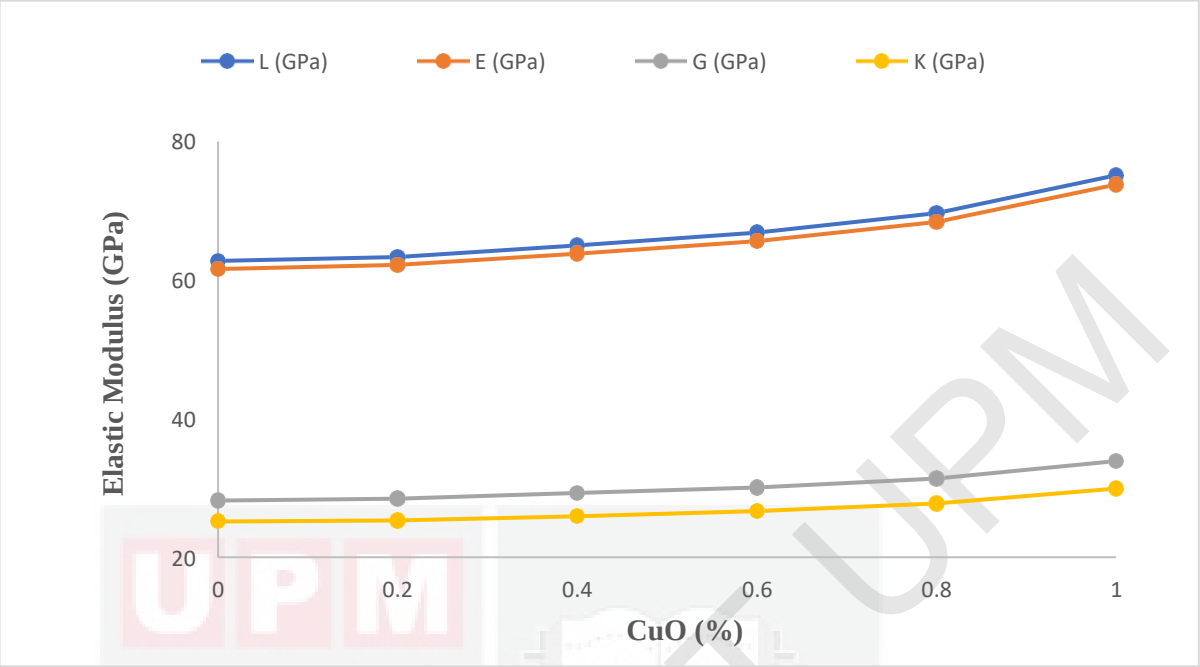

Figure 4.5 Elastic moduli longitudinal (L_{EXP}), shear (G_{EXP}), bulk (K_{EXP}) and Young's (E_{EXP}) modulus of the CuO-Al_2O_3-MgO-Li_2SO_4-P_2O_5 glass system

Table 4.3 shows the experimental values for longitudinal (L), shear (G), bulk (K), Young's (E) modulus, microhardness (H), and Poisson's ratio as a function of CuO content, while **Figure 4.5** shows the experimental values for experimental elastic moduli as a function of CuO content. **Figure 4.5** shows that the longitudinal, shear, Bulk, and Young's modulus values increase in addition with the increase in CuO concentration. The longitudinal modulus increased from 62.78 to 75.13 GPa, the shear modulus increased from 28.20 to 33.90 GPa, the bulk modulus increased from 25.18 to 29.93 GPa, and the Young's modulus increased from 61.58 to 73.77 GPa when CuO was added to the glass system. Variations in shear and longitudinal velocity are caused by changes in the elastic properties and rigidity of glass. Thus, the increase in longitudinal and shear velocities can be attributed to the glass sample's increasing rigidity and hardness (Nidzam *et al.*, 2021).

Additional to this, the behaviors of L_{EXP} and G_{EXP} will have an impact on the bulk (K_{EXP}) and young (E_{EXP}) modules of the system. It is very clear from **Figure 4.4** that increasing the CuO concentration from 0 to 1 mol percent results in a increase in the longitudinal modulus value greater than the shear modulus value. In addition, the actions of L_{EXP} and G_{EXP} will have an effect on the bulk (K_{EXP}) and Young's (E_{EXP}) moduli, respectively, as a result of their interactions. **Table 4.3** shows a comparison of the elastic modulus values, micro hardness (H_{EXP}), and Poisson Ratio (σ_{EXP}) of modified and pure alumina magnesium lithium sulpho phosphate glasses that have been measured and calculated. As can be seen in **Table 4.3**, the elastic moduli values of all of the samples increased as the CuO content increased.

Table 4.3 The experimental results obtained values for elastic moduli, longitudinal (L_{EXP}), shear (G_{EXP}), bulk (K_{EXP}), Young's (E_{EXP}) modulus, Micro Hardness (H_{EXP}) and Poisson's ratio (σ_{EXP}) of the CuO-Al_2O_3-MgO-Li_2SO_4-P_2O_5 glass system

Glass sample	**L_{EXP} (± 0.03GPa)**	**G_{EXP} (± 0.03GPa)**	**K_{EXP} (± 0.03GPa)**	**E_{EXP} (± 0.03GPa)**	**H_{EXP} (± 0.03GPa)**	**σ_{EXP}**
G1	62.78	28.20	25.18	61.58	7.669	0.092
G2	63.35	28.50	25.35	62.19	7.777	0.091
G3	65.00	29.30	25.93	63.82	8.029	0.089
G4	66.83	30.10	26.70	65.62	8.228	0.090
G5	69.67	31.40	27.80	68.39	8.604	0.089
G6	75.13	33.90	29.93	73.77	9.312	0.088

4.4.3 Poisson's ratio (σ) and Micro Hardness (H)

Figure 4.7 and **Table 4.4** shows a decreased value in Poisson's ratio from 0.092 to 0.089 as the CuO content was added. When the CuO content was added, the trend decreased. Poisson's ratio is commonly defined as the lateral to longitudinal strain ratio produced when tensile force is applied (Matori *et al.,* 2017). The addition of CuO leads to a decreased in σ due to an increase in dimensionality.

Table 4.4 shows the computed values of the micro hardness (H_{EXP}) and Poisson's ratio. The deformation of the glass network can be described as microhardness or also can be defined as the stress that glass network need to get the free volume. Higher CuO concentration increased micro hardness from 7.67 to 9.31 GPa as can be seen in **Figure 4.7** due to increase the rigidity of the glass network. Furthermore, increasing microhardness may be associated with the formation of non-bridging oxygens (NBOs), which strengthens the glass network (Nazrin *et al.,* 2018). A similar pattern exists in the variation of ultrasonic velocity with composition, and all elastic moduli variations in glass composition are similar, but the Poisson's ratio decreases with increasing CuO concentration.

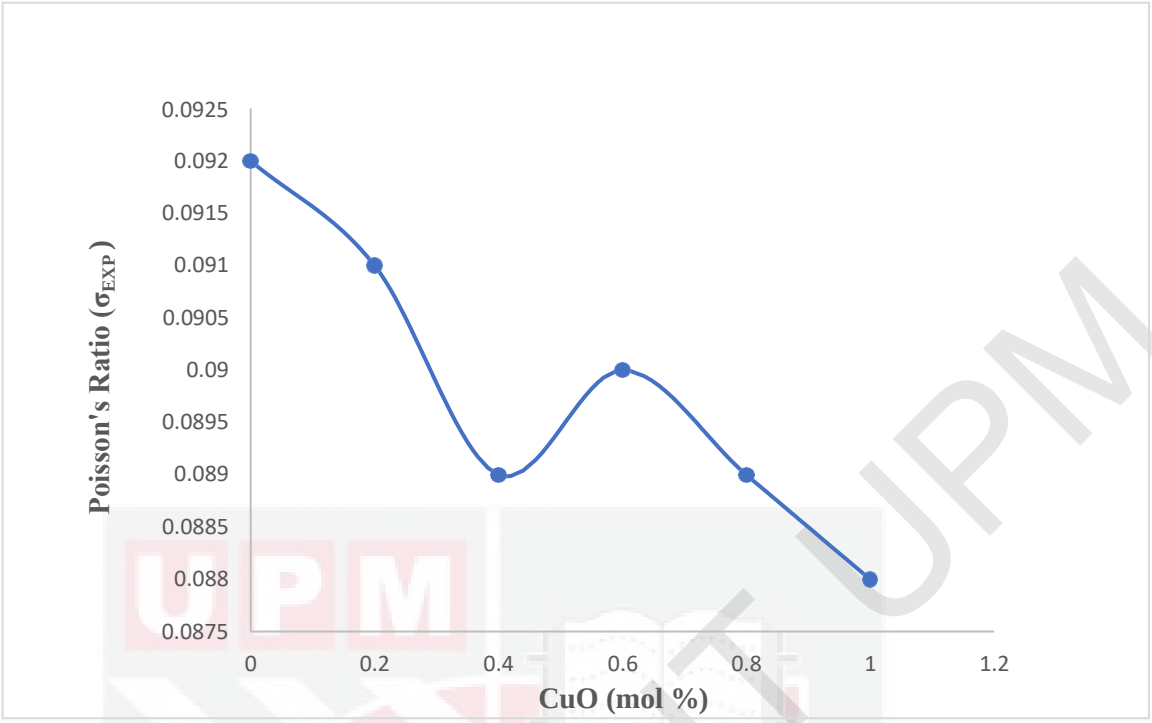

Figure 4.6 Poisson's ratio (σ_{EXP}) of the $CuO\text{-}Al_2O_3\text{-}MgO\text{-}Li_2SO_4\text{-}P_2O_5$ glass system

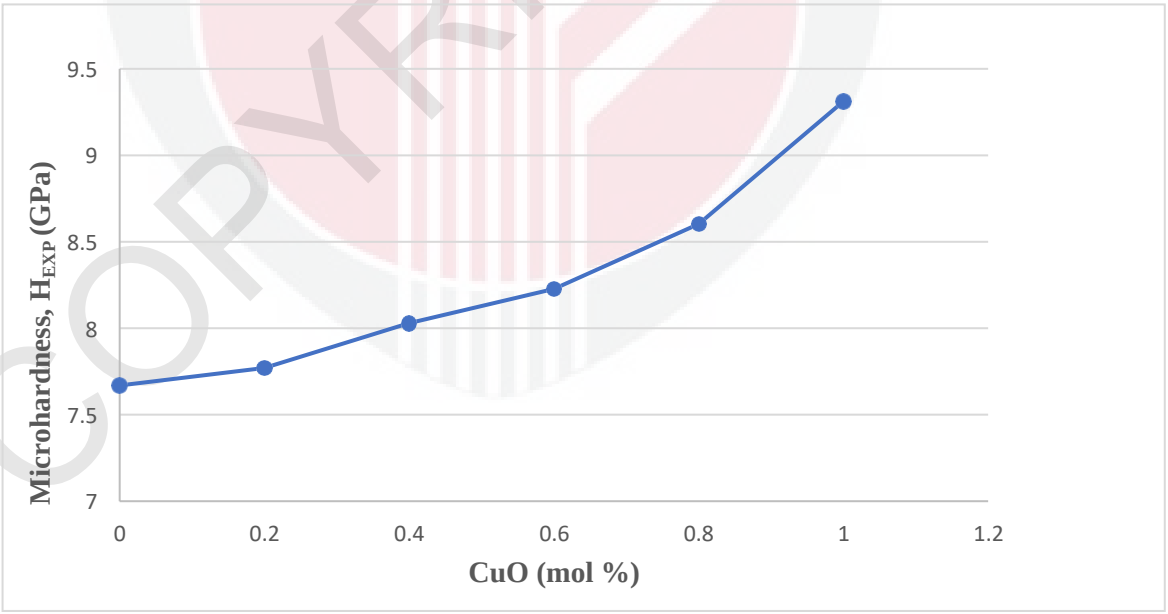

Figure 4.7 Micro hardness (H_{EXP}) of the $CuO\text{-}Al_2O_3\text{-}MgO\text{-}Li_2SO_4\text{-}P_2O_5$ glass system

Figure 4.7 showing the increased in microhardness (H_{EXP}) of the glasses. It shows a reduction in the softening points. The value of micro hardness (H_{EXP}) increased from 7.67 to 9.31GPa as can be seen in **Table 4.4** and **Figure 4.8.** This set of results is highly correlated with the density values discussed in the preceding section, which indicates that the increasing compactness of the glass structure is expected to play an increasingly important role in the enhancement of microhardness. CuO has a large charge, which allows it to be readily incorporated into the amorphous structure and form cross-linking between the phosphate tetrahedra, resulting in the formation of Cu–O–P bonds rather than the more common P–O–P bonds (Ouis *et al.*, 2019).

Table 4.4 Micro hardness (H_{EXP}) and Poisson's ratio (σ_{EXP}) of the CuO-Al_2O_3-MgO-Li_2SO_4-P_2O_5 glass system

Glass sample	**H_{EXP} (± 0.03GPa)**	**σ_{EXP}**
G1	7.67	0.092
G2	7.77	0.091
G3	8.03	0.089
G4	8.23	0.090
G5	8.60	0.089
G6	9.31	0.088

4.5 Theoretical Elasticity Model

4.5.1 Makishima-Mackenzie Model

The elastic moduli calculated using the Makishima and Mackenzie model were used to calculate the dissociation energy per unit volume (G_t) and packing density (V_t) of oxides in a glass composition. (El-Moneim, 2019; Effendy *et al.*, 2020). The model is based on the the molecular weight (M_i), density of oxides (ρ_i), packing density parameter (V_i) and dissociation energy of oxides (G_i) as listed in **Table 4.5**.

The packing density (V_t) and dissociation energy per unit volume (G_t) is presented in **Table 4.6** while **Table 4.7** shows molecular weight (M_i) and elastic moduli (L_m, G_m, K_m, E_m), micro hardness (H_m) and Poisson's ratio (σ_m) according to Makishima-Mackenzie model for CuO-Al_2O_3-MgO-Li_2SO_4-P_2O_5 glass system that has been measured. In this glass composition, the packing density seem to be decreases from 0.932 to 0.914 cm^3/mol^{-1} while dissociation energy per unit volume seem to be increases from 4.391 to 4.412 $kcal/cm^3$. As the dissociation energy per unit volume of all precursor glasses increases, so does the rigidity of the glass, and the elastic moduli of the glass network.

Table 4.5 The molecular weight (M_i), density of oxides (ρ_i), packing density parameter (V_i), dissociation energy of oxides (G_i) of CuO, Al_2O_3, MgO, Li_2SO_4 and P_2O_5.

Oxide	**M_i (± 0.03g mol^{-1})**	**ρ_i (± 0.03g/cm^3)**	**V_i (± 0.03cm^3 mol^{-1})**	**G_i (± 0.03Kcal cm^{-3})**
CuO	79.54	6.31	7.50	59.50
Al_2O_3	101.96	3.95	21.40	131.00
MgO	40.30	3.58	7.60	90.00
Li_2SO_4	109.94	2.22	1.14	34.70
P_2O_5	140.94	2.39	34.80	28.20

Table 4.6 below presents the packing density (V_t) and dissociation energy per unit volume (G_t) of CuO-Al_2O_3-MgO-Li_2SO_4-P_2O_5 glass system that we calculated using Makishima-Mackenzie model. Elastic properties of the glass can be calculated by this model and the result obtained for measured elastic modulus is lower than the experimental value obtained.

Figure 4.8 shows the packing density (V_t) of CuO-Al_2O_3-MgO-Li_2SO_4-P_2O_5 glass system decreased in trend from 0.932 to 0.914 cm^3/mol^{-1}. The replacement of packing density parameter of P_2O_5 with CuO is the reason to this decrement. It is more tightly

packed. The value of dissociation energy per unit volume (G_t) opposite to the packing density with higher concentration of CuO because of the value of dissociation energy of oxides (G_i) of CuO (G_i = 59.5 kcal cm^{-3}) is higher than P_2O_5 (G_i = 28.8 kcal cm^{-3}).

Table 4.6 Packing density (V_t) and dissociation energy per unit volume (G_t) of CuO-Al_2O_3-MgO-Li_2SO_4-P_2O_5 glass system

Glass sample	**V_t (± 0.03cm^3 mol^{-1})**	**G_t (± 0.03Kcal cm^{-3})**
G1	0.932	4.391
G2	0.929	4.937
G3	0.942	4.404
G4	0.920	4.410
G5	0.917	4.412
G6	0.914	4.412

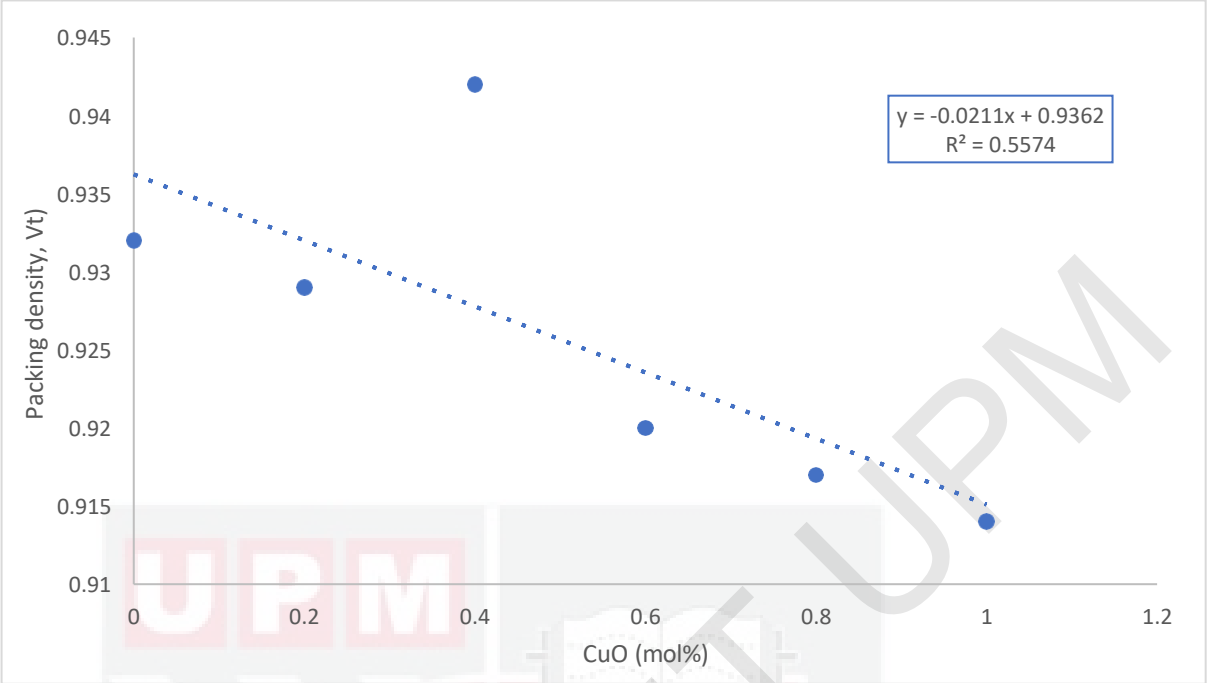

Figure 4.8 The packing density (V_t) variation with CuO mol % for $CuO\text{-}Al_2O_3\text{-}MgO\text{-}Li_2SO_4\text{-}P_2O_5$ glass system

Table 4.7 Molecular weight (M_i), longitudinal modulus (L_m), shear modulus (G_m), bulk modulus (K_m), Young's modulus (E_m), micro hardness (H_m) and Poison's ratio (σ_m) according to Makishima-Mackenzie model for $CuO\text{-}Al_2O_3\text{-}MgO\text{-}Li_2SO_4\text{-}P_2O_5$ glass system

Glass sample	**M_i (± 0.03g mol^{-1})**	**L_m (± 0.03GPa)**	**G_m (± 0.03GPa)**	**K_m (± 0.03GPa)**	**E_m (± 0.03GPa)**	**H_m (± 0.03GPa)**	**σ_m**
G1	118.298	19.657	6.673	7.652	24.83	2.084	0.086
G2	118.173	20.859	7.504	7.891	25.58	2.127	0.084
G3	118.048	22.379	8.254	7.967	26.10	3.116	0.078
G4	117.924	23.688	9.693	8.123	27.91	3.274	0.081
G5	117.798	23.910	10.818	8.694	30.39	3.522	0.078
G6	117.674	28.214	11.741	9.930	35.75	4.110	0.076

The result resulting from Makishima-Mackenzie model is shown as in **Table 4.7** above. The findings demonstrate that the theoretical elastic moduli values are smaller than the values obtained through experimental measurement. It is discovered that, despite the fact that the correlation between theoretical and experimental results is relatively low, the findings indicate a reasonably acceptable agreement in the elastic moduli and micro hardness. These lower values can be attributed to a decrease in packing density, as well as a decrease in molar volume, as well as an increase in the amount of energy dissociated. The longitudinal (L_m) value is increased from 19.657 to 28.241 GPa, shear (G_m) increased from 6.673 to 11.741 GPa, bulk (K_m) increased from 7.652 to 9.930 GPa and Young's (E_m) from 24.83 to 35.75 GPa. Moreover, micro hardness (H_m) value increased from 2.084 to 4.110 GPa and lastly Poisson's ratio (σ_m) decreased from 0.086 to 0.076.

Figure 4.9 until **Figure 4.12** shows the comparison between experimental and the theoretical elastic moduli based on Makishima-Mackenzie model while **Figure 4.13** and **Figure 4.14** illustrated the comparison between experimental and theoretical of micro hardness and Poisson's ratio with an increasing in CuO concentration. As can be seen in the figures, the correlation between experimental and theoretical values is 97.58 % for longitudinal modulus (L_m), 95.43 % for shear modulus (G_m), 98.43 % for bulk modulus (K_m) and 99.56 % for Young's modulus. Whereas the correlation percentage between theoretical and experimental value for micro hardness (H_m) is 93.54 % and lastly for Poisson's ratio (σ_m**)** is 99.65 % respectively. As a result of this finding, the Makishima-Mackenzie model is effective in determining elastic moduli because its correlation percentage is close to 100 %. These shows that the elastic moduli, microhardness, and Poisson's ratio calculated by the Makishima and

Mackenzie model are valid for all of the investigated glass samples, and there is excellent agreement between the calculated and observed values of these parameters.

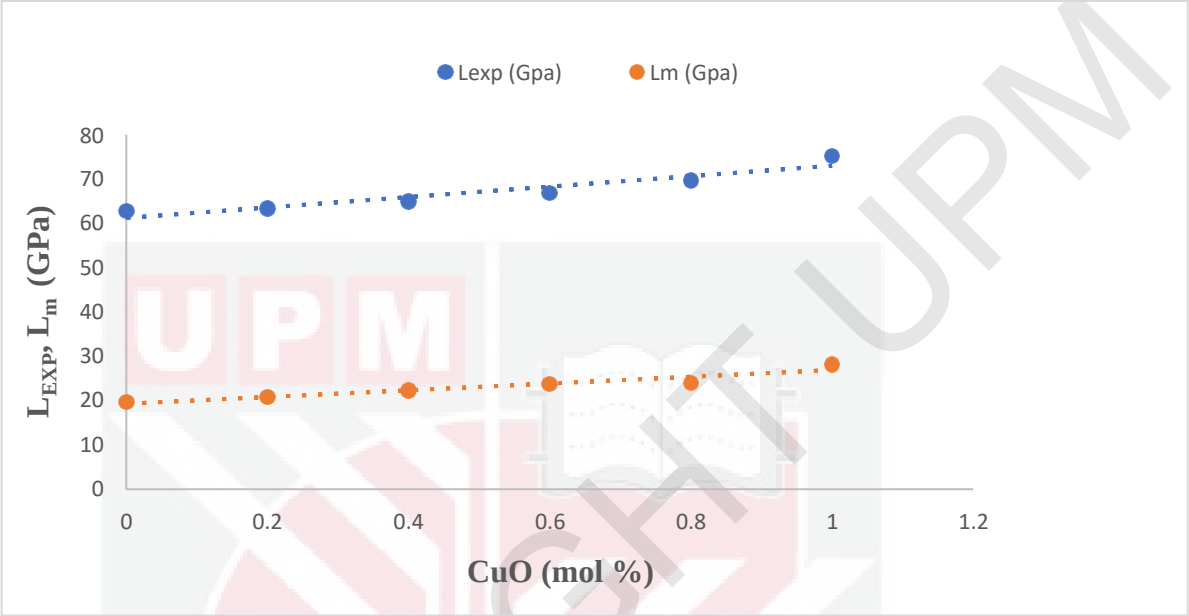

Figure 4.9 Experimental longitudinal modulus (L_{EXP}) and predicted (L_m) value using Makishima-Mackenzie model for CuO-Al_2O_3-MgO-Li_2SO_4-P_2O_5 glass system

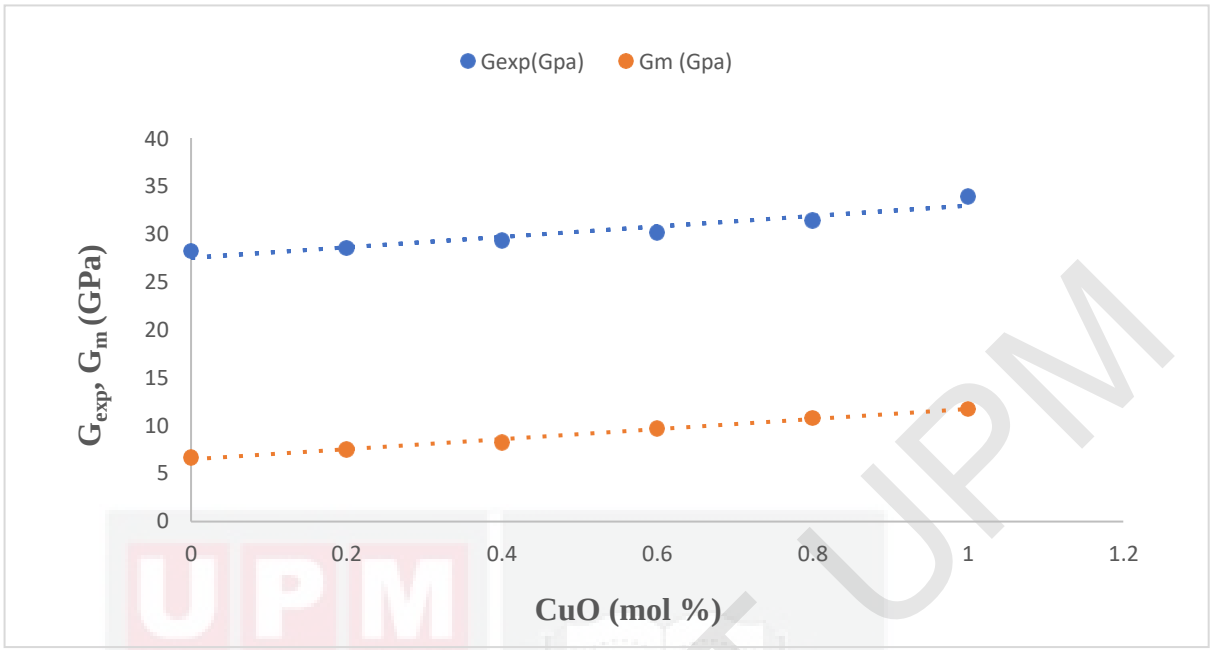

Figure 4.10 Experimental shear modulus (G_{EXP}) and predicted (G_m) value using Makishima-Mackenzie model for CuO-Al_2O_3-MgO-Li_2SO_4-P_2O_5 glass system

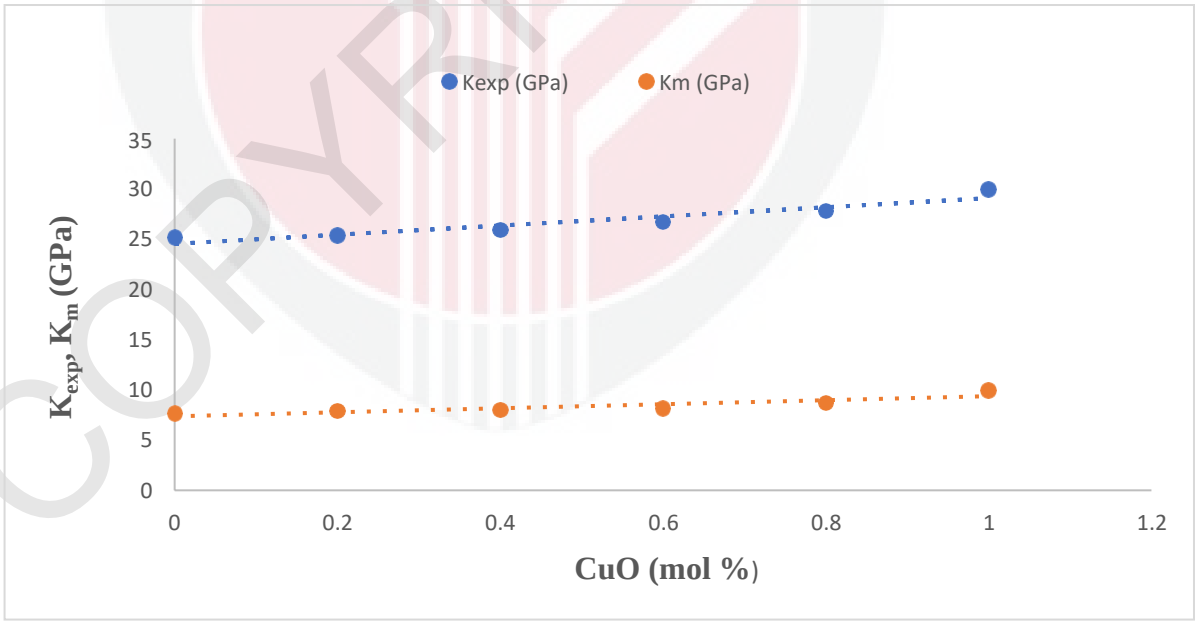

Figure 4.11 Experimental bulk modulus (K_{EXP}) and predicted (K_m) value using Makishima-Mackenzie model for CuO-Al_2O_3-MgO-Li_2SO_4-P_2O_5 glass system

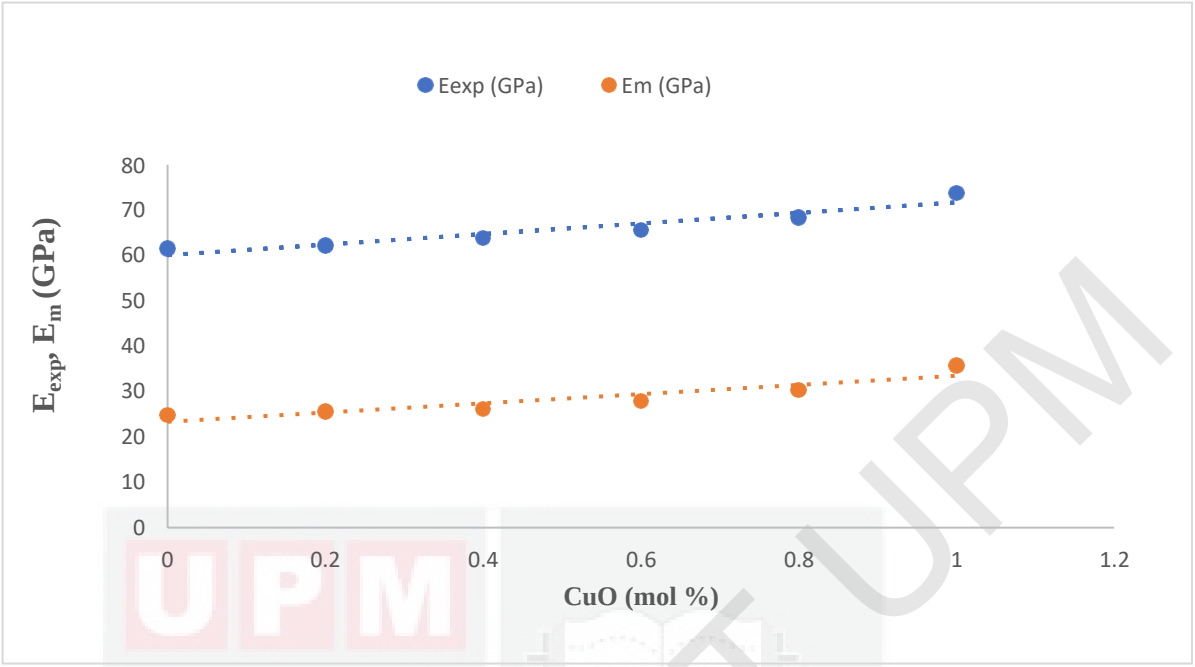

Figure 4.12 Experimental Young's modulus (E_{EXP}) and predicted (E_m) value using Makishima-Mackenzie model for CuO-Al_2O_3-MgO-Li_2SO_4-P_2O_5 glass system

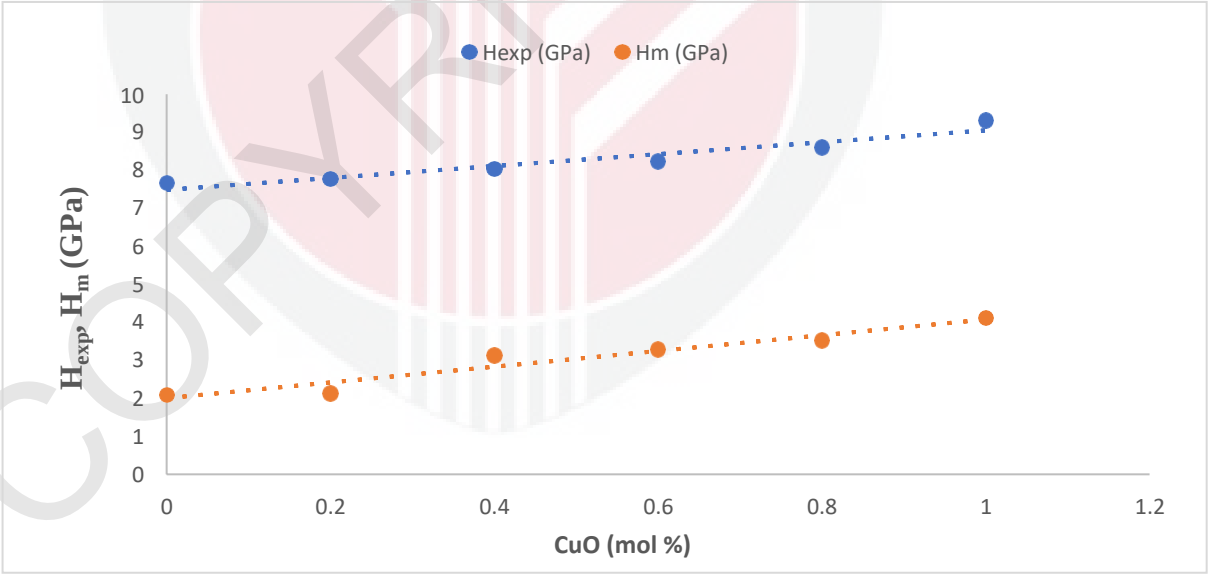

Figure 4.13 Experimental micro hardness (H_{EXP}) and predicted (H_m) value using Makishima-Mackenzie model for CuO-Al_2O_3-MgO-Li_2SO_4-P_2O_5 glass system

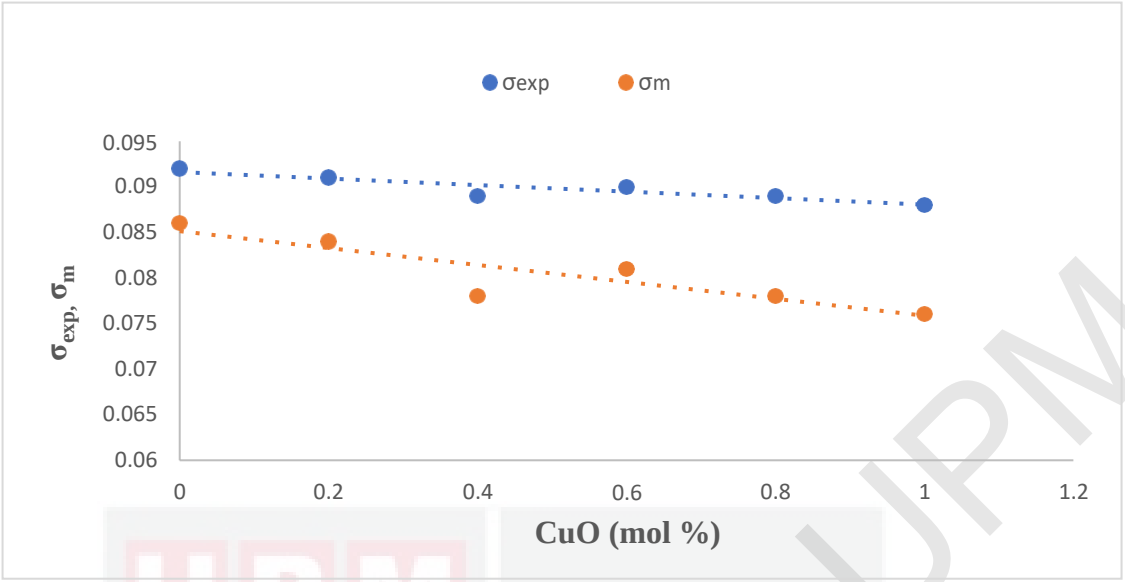

Figure 4.14 Experimental Poisson's ratio (σ_{EXP}) and predicted (σ_m) value using Makishima-Mackenzie model for CuO-Al_2O_3-MgO-Li_2SO_4-P_2O_5 glass system

CHAPTER 5

CONCLUSION AND RECOMMENDATIONS

5.1 Conclusion

In this analysis, the structural and elastic properties of a glass series CuO-Al_2O_3-MgO-Li_2SO_4-P_2O_5 with empirical formula, x(CuO)-5(Al_2O_3)-15(MgO)-20(Li_2SO_4)-60-x(P_2O_5) with

x= 0, 0.2, 0.4, 0.6, 0.8 and 1.0 mol % were demonstrated. Based on the result obtained, there are no sharp peak was observed in the XRD results of the glass system which demonstrate a typical completely amorphous glass structure without absence of crystallization. Moreover, the density and its molar volume of the precursor glass samples both were increased and decrease respectively with addition of CuO content in increasing concentration. Oxygen packing density is decreased when P_2O_5 were substituted with CuO while the value of oxygen molar volume (Vo) is increased advocates that the precursor glasses become more denser dan compact. In addition, the ultrasonic velocities measurement showed that the longitudinal and shear ultrasonic velocities both increase with the increasing of CuO concentration which caused to create more non-bridging oxygens in the network glass system. The value of Poisson's ratio decreased which the rigidity of the glass system is increasing, while micro hardness (H_{exp}) increased as CuO content was added.

Study the effect of CuO to the structural and elastic properties of alumina magnesium lithium sulphophosphate glass system demonstrates that $CuO\text{-}Al_2O_3\text{-}MgO\text{-}Li_2SO_4\text{-}P_2O_5$ glass has a good advantages since high density of the sample and the decrease in molar volume. The glass network of phosphate glasses will be improved because the glass network more NBOs will be produced. Based on the result obtained in this analysis which are its density, molar volume, elastic modulus in experimental and theoretical model (Makishima-Mackenzie model) this $CuO\text{-}Al_2O_3\text{-}MgO\text{-}Li_2SO_4\text{-}P_2O_5$ glass sample appears to be promising for use in the field of sealing and laser glasses also in biomedical glasses.

Lastly, copper alumina magnesium lithium sulphophosphate glass system was synthesized using conventional melt-quenching method and also the effect of CuO to the structural and elastic properties of alumina magnesium lithium sulphophosphate glass system was determined. The correlation between Makishima and Mackenzie model to the elastic properties of alumina magnesium lithium sulphophosphate glass system was investigated.

5.2 Recommendation for Future Research

The present research has successfully investigated the physical, structural, and elastic properties of CuO, which was synthesised by the melt-quenching method from the precursor $CuO\text{-}Al_2O_3\text{-}MgO\text{-}Li_2SO_4\text{-}P_2O_5$ glass system and studied in detail previously. Although the current study's findings suggest that additional work is needed in terms of confirmatory investigations, improvements, as well as other properties

investigations, the findings of the current study indicate that more work is needed in this area. However, there are a few ways to improve for future research:

1) Different kinds of transition metals can be used as a glass modifier such as cobalt (Co^{2+}), sodium (Na+), and zinc (Zn^{2+}).
2) Deeply study on the other theoretical model such as bond compression and artificial neural networks model to predict the elastic moduli of oxide glasses.
3) Studies on other properties such as optical, thermal, electrical, and dielectric properties of CuO-Al_2O_3-MgO-Li_2SO_4-P_2O_5 glass.
4) Further investigation using a variety of preparation methods, such as sol-gel, flux, solid state, and the supercritical water method.

REFERENCES

Abd El-Moneim, A., & Alfifi, H. Y. (2018). Approach to dissociation energy and elastic properties of vanadate and V2O5-contained glasses from single bond strength: Part I. Materials Chemistry and Physics, *207*, 271–281. https://doi.org/10.1016/j.matchemphys.2017.12.057

Abed, H., Damrawi, G. E., Sherbiny, M. E., & Farouk, M. (2021). A new focus on the structure and mechanics of Cuo-modified P2O5-V2O5 glasses. *Journal of Non-Crystalline Solids*, *568*, 120959. https://doi.org/10.1016/j.jnoncrysol.2021.120959

Ahmad, M., Aly, K., Saddeek, Y. B., & Dahshan, A. (2020). Glass transition and crystallization kinetics of NA2O – B2O3 – NB2O5 – BI2O3 Ceramic Glasses. *Journal of Non-Crystalline Solids*, *546*, 120260. https://doi.org/10.1016/j.jnoncrysol.2020.120260

Amarnath Reddy, A., Surendra Babu, S., & Vijaya Prakash, G. (2012). Er3+-doped phosphate glasses with improved gain characteristics for broadband optical amplifiers. Optics Communications, *285*(24), 5364–5367. https://doi.org/10.1016/j.optcom.2012.08.031

Banerjee, S. (2011). *[Functional Materials: Preparation, Processing and Applications [FUNCTIONAL MATERIALS: PREPARATION, PROCESSING AND APPLICATIONS BY Banerjee, S. (Author) Dec-26-2011] By Banerjee, S. (Author) [2011) [Hardcover]*. Elsevier.

Calahoo, C., & Wondraczek, L. (2020). Ionic glasses: Structure, properties and classification. Journal of Non-Crystalline Solids: X, 8, 100054. https://doi.org/10.1016/j.nocx.2020.100054

Chanshetti, U., Shelke, V., Jadhav, S., Shankarwar, S., Chondhekar, T., Shankarwar, A., Sudarsan, V., & Jogad, M. (2011). Density and molar volume studies of phosphate glasses. Facta Universitatis - Series: Physics, Chemistry and Technology, *9*(1), 29–36. https://doi.org/10.2298/fupct1101029c

Da, N., Enany, A., Granzow, N., Schmidt, M., Russell, P., & Wondraczek, L. (2011). Interfacial reactions between tellurite melts and silica during the production of microstructured optical devices. Journal of Non-Crystalline Solids, *357*(6), 1558–1563. https://doi.org/10.1016/j.jnoncrysol.2010.12.032

Elbashar, Y. H., Ali, M. I., Elshaikh, H. A., & El-Din Mostafa, A. G. (2016). Influence of Cuo and al2o3 addition on the optical properties of sodium zinc phosphate glass absorption filters. *Optik*, *127*(18), 7041–7053. https://doi.org/10.1016/j.ijleo.2016.05.008

Elhaes, H., Attallah, M., Elbashar, Y., Al-Alousi, A., El-Okr, M., & Ibrahim, M. (2014). Modeling and optical properties of P2O5–zno–cao–na2O glasses doped with copper oxide. *Journal of Computational and Theoretical Nanoscience*, *11*(10), 2079–2084. https://doi.org/10.1166/jctn.2014.3608

El-Moneim, A. A. (2019). Elastic Moduli and Poisson's ratio prediction in borate-based PBO-B2O3-V2O5 and li2o-zno-B2O3 glass systems. *Journal of Non-Crystalline Solids*, *514*, 69–76. https://doi.org/10.1016/j.jnoncrysol.2019.03.035

Filho, J. C., Zilio, S. C., Messias, D. N., Pilla, V., Almeida Silva, A. C., Dantas, N. O., & Andrade, A. A. (2020). Effects of aluminum substitution by potassium in the P2O5–al2o3–Na2O–K2O Phosphate Glasses. *Journal of Alloys and Compounds*,

Granados, L., Morena, R., Takamure, N., Suga, T., Huang, S., McKenzie, D. R., & Ho-Baillie, A. (2021). Silicate glass-to-glass hermetic bonding for encapsulation of next-generation optoelectronics: A Review. *Materials Today*, *47*, 131–155. https://doi.org/10.1016/j.mattod.2021.01.025

Hémono, N., & Muñoz, F. (2010). Dissolution of SO3 within a lithium phosphate glass network and structure–property relationships. http://hdl.handle.net/10261/64189

Jaccani, S. P., Sundararaman, S., & Huang, L. (2018). Understanding the structural origin of intermediate glasses. Journal of the American Ceramic Society. doi:10.1111/jace.15935

LEE, S., KIM, J., & SHIN, D. (2007). Modification of network structure induced by glass former composition and its correlation to the conductivity in lithium borophosphate glass for solid state electrolyte. Solid State Ionics, *178*(5–6), 375–379. https://doi.org/10.1016/j.ssi.2007.01.011

Lim, H., Jung, J. H., Park, Y. M., Lee, H. N., & Kim, H. J. (2018). High-performance aqueous rechargeable sulfate- and sodium-ion battery based on polypyrrole-MWCNT core-shell nanowires and Na0.44MnO2 nanorods. Applied Surface Science, *446*, 131–138. https://doi.org/10.1016/j.apsusc.2018.02.021

Mahan, G. D. , Douglas, . Ronald Walter and Zallen, . Richard (2019, July 31). Amorphous solid. Encyclopedia Britannica. https://www.britannica.com/science/amorphous-solid

Matori, K. A., Sayyed, M. I., Sidek, H. A. A., Zaid, M. H. M., & Singh, V. P. (2017). Comprehensive study on physical, elastic and shielding properties of lead zinc phosphate glasses. *Journal of Non-Crystalline Solids*, *457*, 97–103. https://doi.org/10.1016/j.jnoncrysol.2016.11.029

MINAMF, T., & MACKENZIE, J. D. (1977). Thermal Expansion and Chemical Durability of Phosphate Glasses. Journal of the American Ceramic Society, *60*(5–6), 232–235. https://doi.org/10.1111/j.1151-2916.1977.tb14113.x

Morshidy, H. Y., Sadeq, M. S., Mohamed, A. R., & EL-Okr, M. M. (2020). The role of CUCL2 in tuning the physical, structural and optical properties of some al2o3–B2O3 glasses. *Journal of Non-Crystalline Solids*, *528*, 119749. https://doi.org/10.1016/j.jnoncrysol.2019.119749

NIDZAM, N. N. S., Sharma, A., Jufa, M. S., Izzaty, M. K., & Boukhris, I. (2021). Mechanical and Radiation Shielding properties of CuO doped TeO2-B2O3 Glass System.

Nie, H., Zhang, J., Qi, Y., Wang, Z., Lin, H., & Jiang, S. (2015). Influence of composition on the structure and properties of SrO–Sb2O3–P2O5 low-melting sealing glasses. Materials Science-Poland, *33*(4), 862–866. https://doi.org/10.1515/msp-2015-0117

Oueslati-Omrani, R., & Hamzaoui, A. H. (2020). Effect of zno incorporation on the structural, thermal and optical properties of phosphate based silicate glasses. Materials Chemistry and Physics, 242, 122461. https://doi.org/10.1016/j.matchemphys.2019.122461

Ouis, M. A., Taha, M. A., El-Bassyouni, G. T., & Azooz, M. A. (2019). Thermal, mechanical and electrical properties of lithium phosphate glasses doped with copper oxide. *Bulletin of Materials Science*, *42*(5). https://doi.org/10.1007/s12034-019-1897-y

Phillips G.C. (1991) Structure of Glass. In: A Concise Introduction to Ceramics. Springer, Dordrecht. https://doi.org/10.1007/978-94-011-6973-8_11

Plucinski, M., & Zwanziger, J. (2015). Topological constraints and the Makishima–Mackenzie model. *Journal of Non-Crystalline Solids*, *429*, 20–23. https://doi.org/10.1016/j.jnoncrysol.2015.08.029

Prasad, S., Srinivasa Reddy, M., Ravi Kumar, V., & Veeraiah, N. (2007b). Specific features of photo and thermoluminescence of Tb3+ ions in BaO–M2O3 (M=Ga, Al, In)–P2O5 glasses. Journal of Luminescence, *127*(2), 637–644. https://doi.org/10.1016/j.jlumin.2007.03.011

Saddeek, Y. B., Shaaban, K. H. S., Aly, K. A., Farag, R. S., & Uosif, M. A. M. (2015). Studying effect of SiO2 on elastic properties of glasses based on environmental tailings using a nondestructive ultrasonic method. Int J New Hor Phys, *2*(2), 53-57.

Sallam, O. I., Abdeldaym, A., & Ezz-Eldin, F. M. (2020). Synthesis and physical characterization of gamma irradiated cadmium phosphate glass modified by copper oxide. *Materials Chemistry and Physics*, *252*, 123241. https://doi.org/10.1016/j.matchemphys.2020.123241

Saloumi, N., El Bouchti, M., Tamraoui, Y., Manoun, B., Hannache, H., & Cherkaoui, O. (2019). Structural, chemical and mechanical properties of phosphate glass fibers. *Journal of Non-Crystalline Solids*, *522*, 119587. https://doi.org/10.1016/j.jnoncrysol.2019.119587

Sayyed, M. I., Issa, S. A. M., Tekin, H. O., & Saddeek, Y. B. (2018). Comparative study of gamma-ray shielding and elastic properties of $BaO–Bi_2O_3–B_2O_3$ and $ZnO–Bi_2O_3–B_2O_3$ glass systems. *Materials Chemistry and Physics*, *217*, 11-22.

Scholz, F. (2011). The electrochemistry of particles, droplets, and vesicles – the present situation and future tasks. Journal of Solid State Electrochemistry, *15*(7–8), 1699–1702. https://doi.org/10.1007/s10008-011-1318-7

Sekhar, A. V., Pavić, L., Moguš-Milanković, A., Purnachand, N., Reddy, A. S. S., Raju, G. N., & Veeraiah, N. (2020). Dielectric characteristics, dipolar relaxation dynamics and ac conductivity of CuO added lithium sulpho-phosphate glass system. Journal of Non-Crystalline Solids, *543*, 120157. https://doi.org/10.1016/j.jnoncrysol.2020.120157

Sułowska, J., Wacławska, I., & Szumera, M. (2012). Effect of copper addition on glass transition of silicate–phosphate glasses. *Journal of Thermal Analysis and Calorimetry*, *109*(2), 705–710. https://doi.org/10.1007/s10973-012-2328-0

Varshneya, A. K. (2016, May 10). Industrial glass. Encyclopedia Britannica. https://www.britannica.com/topic/glass-properties-composition-and-industrial-production-234890#ref608298

Yuntian Zhu. MSE200 Lecture19(CH.11.6,11.8)Ceramics. *19*, 1–21 https://people.engr.ncsu.edu/ytzhu/Class-Teaching/MSE200/Lecture19-Nov23.pdf

Zaid, M. H. M., Matori, K. A., Nazrin, S. N., Azlan, M. N., Hisam, R., Iskandar, S. M., Yusof, N. N., Hila, F. C., & Sayyed, M. I. (2021). Synthesis, mechanical characterization and photon radiation shielding properties of zno–al2o3–bi2o3–B2O3 glass system. *Optical Materials*, *122*, 111640. https://doi.org/10.1016/j.optmat.2021.111640

Zamyatin, O., Churbanov, M., Medvedeva, J., Gavrin, S., Zamyatina, E., & Plekhovich, A. (2018). Glass-forming region and optical properties of the TeO 2 – ZnO – NiO system. Journal of Non-Crystalline Solids, *479*, 29–41. https://doi.org/10.1016/j.jnoncrysol.2017.10.005

Zhang, L., Qu, Y., Wan, X., Zhao, J., Zhao, J., Yue, Y., & Kang, J. (2020). Influence of rare earth oxides on structure, dielectric properties and viscosity of alkali-free aluminoborosilicate glasses. Journal of Non-Crystalline Solids, *532*, 119886. https://doi.org/10.1016/j.jnoncrysol.2020.119886